Metal-Chelating Peptides Derived from Sunflower Meal Protein: Preparation, Isolation, Identification, and Antioxidant Properties

Jairo Andrés Camaño Echavarría, Christelle Mathé, Philippe Arnoux, Loïc Stefan, Cédric Paris, Katalin Selmeczi, Chibuike Udenigwe, Laetitia Canabady-Rochelle

Metal-Chelating Peptides Derived from Sunflower Meal Protein: Preparation, Isolation, Identification and Antioxidant Properties

Jairo Andrés Camaño Echavarría[1*], Christelle Mathe[1], Philippe Arnoux[1], Loïc Stefan[2], Cédric Paris[3], Katalin Selmeczi[4], Chibuike Udenigwe[5], Laetitia Canabady-Rochelle[1*]

*Corresponding authors:

E-mail:

jairo-andres.camano-echavarria@univ-lorraine.fr

laetitia.canabady-rochelle@univ-lorraine.fr

[1]Université de Lorraine, CNRS, LRGP, F-54000 Nancy, France

[2]Université de Lorraine, CNRS, LCPM, F-54000 Nancy, France

[3]Université de Lorraine, LIBIO, F-54000 Nancy, France

[4]Université de Lorraine, CNRS, L2CM, F-54000 Nancy, France

[5]School of Nutrition Sciences, University of Ottawa, Ottawa, Ontario, K1H 8M5, Canada

Abstract

Sunflower meal, a by-product of sunflower seed oil extraction, contains approximately 30-50 % proteins. Recognized for its high protein content and bioavailability, it is suitable for bioactive peptides production. Yet, research exploring the potential of sunflower proteins for generating metal-chelating peptides (MCPs) is sparse. Therefore, this study aimed to evaluate sunflower meal as a protein source to produce metal-chelating peptides. After protein extraction to obtain a sunflower protein isolate, single and sequential enzymatic treatments were applied to produce hydrolysates using Protamex® (Prot) and Protamex followed by Flavourzyme® (Prot+Flav), respectively. Upon sequential treatment, effectively large number of peptide bonds were cleaved, releasing mainly small-sized peptides. Prot hydrolysates exhibited the highest Fe^{2+}-chelating properties, inhibition of Cu^{2+}-induced reactive oxygen species (ROS) production, and ABTS scavenging activities. Besides, sequential hydrolysis with both enzymes enhanced the inhibition of Fe^{3+}-induced ROS production and the reducing power. The Cu^{2+}-chelating peptides present in hydrolysates were separated using immobilized metal ion affinity chromatography (IMAC-Cu^{2+}) and identified by LC-MS/MS analysis. MS/MS analysis of enriched Cu^{2+}-binding peptide fractions unveiled twenty-nine potential His-containing MCPs from SMPI hydrolysate. The molecular weight of Cu^{2+}-identified peptides ranged from 0.8-1.7 kDa, with the larger-sized peptides (> 1 kDa) presenting the most effective bioactive properties. His, Glu and Asp residues were crucial for metal-chelating and antioxidant properties. Due to their high potential to bind Cu^{2+}, Fe^{2+} and Fe^{3+}, sunflower meal peptides could serve as potential MCPs candidates for use as food or pharmaceutical agents to prevent metal-induced oxidation and related-diseases.

Key words: bioactive peptides, protein hydrolysate, enzymatic hydrolysis, sunflower seed, peptide-metal complex

1. Introduction

Sunflower (*Helianthus annuus* L.) is the 3rd ranking oilseed after soybean and rapeseed in terms of volumes with a worldwide production of 47 million metric tons in 2023.[1] Obtained after sunflower seed oil extraction, the meal residue contains approximately 30-50 % proteins. Due to its high protein content and bioavailability, sunflower meal is a potential source of biomaterials for a broad range of food applications, particularly for bioactive peptides production. Initially encrypted within primary protein sequence under an inactive form, bioactive peptides can be released by proteolysis.[2] They have gained considerable attention owing to their diverse health benefits. Sunflower meal protein produced hydrolysates were reported to possess immune-modulating[3], angiotensin-converting inhibiting[4], antioxidant and anti-inflammatory activities.[5]

In food protein hydrolysates, metal-chelating peptides (MCPs) can be generated from a variety of protein sources, such as milk, eggs and fish.[2] Based on a sustainable development perspective and utilization of biological resources, many studies have focused on by-product and plant proteins. This presents tremendous potential for the production of MCPs due to their high protein content and their potential high-added value after proteolysis.[5] Several plant-based proteins such as rapeseed[6], defatted walnut flake[7] and chia seed[8] were reported for producing zinc, iron and copper-chelating peptides, respectively. Meanwhile, MCPs were rarely investigated in sunflower protein hydrolysate.[9-11]

MCPs are characterized by their capacity to form coordination complexes with metals such as Ca^{2+}, Zn^{2+}, $Fe^{2+/3+}$ and Cu^{2+}. These biofunctional peptides have widely been proposed as potent alternatives to combat metal-related diseases.[2]. Indeed, MCPs can be used as delivery agents for enhancing the stability, absorption, and bioavailability of minerals.[12] Additionally, by complexing Fe^{2+} and Cu^{2+}, MCPs could efficiently mitigate oxidative damage associated with chronic diseases. Indeed, iron and copper ions have the potential to catalyze the production of reactive oxygen species (ROS) *via* the Fenton and Haber Weiss reactions, triggering radical chain reactions that can damage biomolecules and thus, induce various diseases (degenerative, neurological, cardiovascular and cancer).[13]

MCPs can be separated using immobilized metal ion affinity chromatography (IMAC). This separation technique is based on the affinity of some peculiar amino acids (AA) residues present in peptides for some transition metal ions (*e.g.,* Cu^{2+}, Ni^{2+} or Co^{2+}) immobilized onto the chromatographic phase. Due to its high selectivity, high binding capacity and high recovery, IMAC is a powerful purification methodology for MCPs in food-derived protein hydrolysates.[6] Zu et al.[14] and Xie et al.[6] purified and identified zinc-chelating peptides

from wheat germ and rapeseed hydrolysates, respectively, using IMAC-Zn^{2+}. More recently, Bao et al.[10] used IMAC-Ca^{2+} to purify calcium-binding peptides from sunflower meal hydrolysates, whereas Latha et al.[8] separated IMAC-Cu^{2+} and identified metal-chelating peptides from chia seed proteins.

To the best of our knowledge, there are only a few reports on the use of sunflower meal for producing MCPs.[9-11]. Although Cu^{2+}-chelating peptides were produced from sunflower meal protein hydrolysate[11], the peptide sequences or their metal-related antioxidant activities were not identified. Besides, there are no reports on purification and identification of Cu^{2+}-chelating peptides from sunflower meal protein hydrolysate generated from sequential enzymatic treatment. In contrast to previous studies that have primarily reported the antioxidant properties of sunflower protein hydrolysates, our work provides a comprehensive and in-depth characterization of their metal-chelating profile. By combining a sequential enzymatic hydrolysis approach with physicochemical characterization, peptide identification using IMAC-Cu^{2+} followed by MS/MS, and antioxidant activity assessment, this work provides novel insights into the metal-chelating profile of this by-product. This study not only highlights the biofunctional potential of these peptides, but also establishes relationship between their sequences and metal-related antioxidant properties.

2. Materials & Methods

2.1. Chemicals and Equipment

Sunflower meal (SM) was provided by SAS IMPROVE (Dury, France). Protamex® (Prot, protease from *Bacillus* sp., ≥ 1.5 U/g), Flavourzyme® (Flav, protease from *Aspergillus oryzae*, ≥ 500 U/g), 37 % hydrochloric acid (HCl), 97 % sulfuric acid (H_2SO_4), nitric acid (HNO_3), ammonium bicarbonate, *o*-phthaldialdehyde (OPA), N,N-dimethyl-2-mercaptoethyl ammonium, sodium tetraborate, sodium dodecyl sulfate, glycine, monobasic potassium phosphate, and all the antioxidant testing chemicals, including ethylenediaminetetraacetic acid (EDTA), carnosine, 3-(2-Pyridyl)-5,6-diphenyl-1,2,4-triazine-p,p′-disulfonic acid monosodium salt hydrate 97% (ferrozine), ferrous chloride solution ($FeCl_2$) 2,2′-azinobis (3-ethylbenzothiazoline-6-sulfonic acid) diammonium salt (ABTS), 6-hydroxy-2,5,7,8-tetramethylchroman-2-carboxylic acid (Trolox®), potassium persulfate, potassium ferricyanide, trichloroacetic acid (TCA), ferric chloride ($FeCl_3$), iron(III) ferrocyanide $Fe_4[Fe(CN)_6]_3$ (Prussian blue), ascorbic acid were purchased from Sigma–Aldrich (St Louis, MO, USA). All the other reagents were analytical grade and purchased from VWR

International (Atlanta, USA): copper (II) sulfate pentahydrate, potassium sulfate, sodium phosphate monobasic-NaH_2PO_4, sodium phosphate dibasic-Na_2HPO_4, Na2HPO4·12H2O, sodium chloride, 99% HEPES ($C_8H_{18}N_2O_4S$), and copper (II) chloride hydrate. The PolyEthylenGlycol molecular standards (PEG: 200, 600, 1000, 3000 and 8000 Da) were purchased from Sigma–Aldrich (St Louis, MO, USA).

All the spectrophotometric measurements were performed using a MRX Multiskan Go microplate reader (ThermoFicher Scientific, Vantaa, Finland) and 96-well microplates NunclonTM delta surface (Thermo scientific, Roskilde, Denmark).

2.2. Production of Sunflower meal protein isolate

Sunflower meal protein isolate (SMPI) was obtained using the method reported by Kalpana et al.[15] based on NaCl extraction to solubilize the majority of globulins proteins, and avoid undesirable colour change of the extract due to the oxidation of phenolic compounds and their interaction with proteins. Sunflower meal (30 g) was dissolved into a 1:10 (g/ mL) meal-to-ultra-pure water ratio, added with 10 % (w/v) of NaCl. Then, this former solution was stirred (60 minutes, 40 °C, and pH 6). After solubilization, the samples were cloth filtrated in order to remove solidified residual fibrous. The resulting solution was centrifuged (Centrifuge Universal 320, Hettich, Tuttlingen, Germany) for 10 minutes, at 20 °C and 3,300 g. Afterward, the resulting supernatant composed of solubilised proteins was recovered and filtrated by vacuum filtration to remove the salt residues remaining from solubilisation. The filtrated supernatant was precipitated by adjusting the pH at 4.5 within 10 min, corresponding to the isoelectric point of sunflower proteins.[9] This suspension was kept for 30 minutes at room temperature (25 ºC), and then centrifuged (3 300 g, 10 minutes, 20 °C). The pellet was finally dried using a convective oven (Thermo ScientificTM, USA) at 55 °C overnight. SMPI was stored at -20 °C until further use.

2.3. Proteolysis

Enzymatic hydrolysis. Sunflower meal protein isolate hydrolysates were obtained as previously described with some modification.[16] First, SMPI was dissolved in 250 mL of 50 mM ammonium bicarbonate buffer solution, and then hydrolysed with Protamex® (Prot), Flavourzyme® (Flav), and Protamex® followed by Flavourzyme® (Prot+Flav) using their optimal conditions, respectively. Hydrolysis parameters were as follows: 2 % (w/v) SMPI concentration, 1 % (w/w) enzyme/substrate ratio, pH 8, 2 h, and 55 ºC for Protamex® while pH 7, 2 h, and 55 ºC were used for Flavourzyme®. Upon hydrolysis, pH was maintained at the desired values by adding 5 M NaOH. After each hydrolysis step, each protease was heat inactivated (95 ºC, 15 min). In sequential

133 treatment, Protamex® was inactivated just before Flavourzyme® treatment. Then, hydrolysates were
134 centrifuged (10 000 g, 15 min, 25 ºC) and the whole hydrolysates fractions were freeze-dried (LABCONCO,
135 Kansas City, USA) and stored at −20 °C for further analysis.

136 Ultrafiltration. Considering our initial results, the two hydrolysates with the highest degree of hydrolysis (Prot
137 and Prot+Flav) were further dissolved (250 mL; 20 mg/mL in ultrapure water) and submitted to ultrafiltration
138 under magnetic stirring and 5 bar of nitrogen pressure.[17] The ultrafiltration unit (UF stirred cell 47-mm system
139 XFUF04701; Millipore, Molsheim, France) was initially equipped with a 10-kDa molecular weight cut-off
140 membrane (MWCO), followed by a 1-kDa MWCO membrane (Millipore, Billerica, USA), conditioned
141 according to the manufacturer's specification, before ultrafiltration. The 10-kDa MWCO membrane was used
142 as a first step to remove larger peptides, prevent potential fouling and improve the efficiency of the subsequent
143 1-kDa MWCO ultrafiltration. This sequential ultrafiltration approach facilitated the effective separation of
144 low-molecular-weight peptides while maintaining optimal membrane performance. The ultrafiltrated fractions
145 of hydrolysates (≤ 1 kDa Prot and ≤ 1 kDa Prot+Flav fractions) were freeze-dried and kept at −20 °C until
146 further analysis.

147 **2.4. Physicochemical characterization**

148 **2.4.1. OPA quantification and degree of hydrolysis**

149 The peptide concentration expressed as mmol equivalent of primary amine groups per gram of hydrolysate
150 (mmol eq. NH_2/g) was evaluated by *o*-phthaldialdehyde (OPA) quantification as previously reported.[13] The
151 degree of hydrolysis (DH) was determined exclusively for the whole hydrolysates (non-ultrafiltrated ones)
152 through OPA quantification and expressed as the ratio of free amino groups present in the hydrolysate to the
153 total amino groups present in the sample. The latter was derived from the complete hydrolysis of sunflower
154 protein (6 N HCl, ratio 1:1 w/v, 130 °C, 24 h), with the assumption that all peptide bonds of the protein were
155 cleaved during acid digestion.[16] The DH was determined by the **Equation 1**.

$$\text{Degree of hydrolysis (\%)} = \left[\frac{\text{NH}_2\,\text{x} - \text{NH}_2\,0}{\text{NH}_2\,\text{T} - \text{NH}_2 0}\right] \text{x } 100 \quad (1)$$

156

157 Where: NH_2 X is number of free-NH_2 groups at final time of enzymatic hydrolysis, NH_2 0 is number of free-
158 NH_2 groups before hydrolysis, and NH_2 T is NH_2 after complete hydrolysis.

2.4.2. Molecular weight distribution

2.4.2.1. SDS-PAGE profile

The molecular weight (MW) profile of SM, SMPI and SMPI hydrolysates were studied using sodium dodecyl sulphate polyacrylamide gel electrophoresis (SDS-PAGE), following the procedure described by Zilic et al.[18] in a Mini-Protean tetra cell electrophoresis system (Bio-Rad Laboratories, Hercules, USA). Samples were prepared at 20 mg/mL in ultrapure water and the solubilized protein solutions were mixed at a 1:4 (v/v) ratio with sample buffer. This sample buffer consisted of 0.5 M Tris-HCl, pH 6.8, with 10% (w/v) SDS, 50% (v/v) glycerol, and 0.05% (w/v) bromophenol blue along with 0.5% (w/v) 2-mercaptoethanol as a reducing agent. These mixtures were heated at 100 °C for 5 minutes. Subsequently, 10 µL of each sample (equivalent to 40 µg of protein) or MW markers (Catalog No: 26619, Thermo Scientific™, Vilnius, Lithuania; range: 10–250 kDa) were loaded onto the polyacrylamide gel, consisting in a 7.5 % separation gel and a 5 % stacking gel.[18] Electrophoresis was carried out at a voltage of 120 V for 15 minutes, followed by 180 V for 1 hour. After electrophoresis, the gel was stained for 1 hour using a solution containing 0.16% (w/v) Coomassie blue R-250, 7.5% (v/v) acetic acid, and 5% (v/v) ethanol. Then, the gel was destained for 1 hour using a solution of 30% (v/v) ethanol and 7.5% (v/v) acetic acid.

2.4.2.2. Size exclusion chromatography

The molecular weight (MW) distribution of the whole hydrolysates (Prot and Prot+Flav) and their ≤ 1 kDa ultrafiltrates (≤ 1 kDa Prot and ≤ 1 kDa Prot+Flav) was analyzed using size-exclusion chromatography (SEC) with a 515 HPLC pump (Waters, Milford, MA, USA), a degasser, and a RID 10-A Shimadzu detector, as previously described.[16] The system featured a Phenomenex PolySep-GFC-P 2000 column (300 × 7.8 mm - 8 µm – 200 A - separation range 100 Da – 10 kDa) safeguarded by a guard column (35 × 7.8 mm) linked to a Phenomenex PolySep-GFC-P 1000 column (300 × 7.8 mm - 8 µm – 100 A - separation range 20 Da – 3 kDa). The four previous hydrolysates (5 mg/mL) were loaded (200 µL) and eluted using an aqueous buffer containing 0.1 M sodium nitrate ($NaNO_3$) and 0.2 % (w/v) sodium azide (NaN_3) at a flow rate of 0.7 mL/min at room temperature (25 ºC). The polyethylene glycol (PEG) standard solutions (200, 600, 1000, 3000, and 8000 Da) were similarly injected for SEC calibration. The chromatograms were analyzed using ASTRA® software (Wyatt Technology, Goleta, USA).

2.5. Metal-chelating peptides characterization

2.5.1. Antioxidant activities

2.5.1.1. Ascorbate tests

The ability of hydrolysates to inhibit the ROS generation catalyzed by transition metals (*i.e.,* Cu^{2+}, Fe^{3+}) was investigated by the ascorbate test. In the presence of oxygen, these metals are able to catalyze the ascorbate oxidation and the metal-catalyzed Fenton-type reaction to produce ROS ($O_2^{\bullet-}$, H_2O_2 and $OH^{\bullet}$).[19] In this assay, Cu^{2+} and Fe^{3+} are reduced into Cu^{+} and Fe^{2+} by ascorbate, respectively. Yet, the resulting metal species are unstable and easily oxidized back to Cu^{2+} and Fe^{3+} forms, following the redox cycle of the metal ions.[20] Ascorbate ($AscH^-$) solution was prepared at 5 mM using 50 mM HEPES buffer at pH 7.4. Stock solution of Cu^{2+} and Fe^{3+} were prepared at 2 mM using $CuCl_2$ (in ultrapure water) and $FeCl_3$ (in 0.1 M HNO_3 acidic solution to maintain the Fe^{3+} in solution). EDTA (positive control in Cu^{2+} assay, and negative control in Fe^{3+} assay), and deferoxamine (DFO, positive control in Fe^{3+} assay) were prepared at 2 mM in order to reach a final concentration of the components at 100 µM, with 1: 1: 1 $AscH^-$: ligand: Cu^{2+}/Fe^{3+} ratio, whereas, SMPI hydrolysates were prepared at 5 mM (eq NH_2 according to OPA assay), with 1: 5: 1 $AscH^-$: ligand: Cu^{2+}/Fe^{3+} ratio. The reaction was initiated by the introduction of ascorbate, and the kinetic study of the ascorbate concentration was carried out by following the absorbance at 265 nm.[19] The results were reported as ascorbate consumed after 2 and 10 min for Cu^{2+} and Fe^{3+}, respectively (ε = 14 500 M^{-1} cm^{-1}). Indeed, ascorbate consumption has a direct correlation with the levels of Cu^{2+} and Fe^{3+} in solution, which can be complexed in the presence of hydrolysates/positive controls. Note that all the measurements were carried out in triplicate.

2.5.1.2. Ferrozine test

The Fe^{2+}-chelating ability of hydrolysates was determined by ferrozine test as previously reported using EDTA (0-0.04 mg/mL) as positive control.[21] Briefly, 7.5 µL of $FeCl_2$ (2 mM) was mixed with 277.5 µL of control or hydrolysate solution (0 to 1 mg/mL in ultrapure water), followed by the addition of 15 µL of ferrozine solution (5 mM) after a 3-minute incubation at room temperature (25 ºC). The mixture was allowed to stand for 10 minutes after shaking. The absorbance of the solution was measured at 562 nm. The iron-chelating activity of the hydrolysates was determined by the **Equation 2**.

$$\text{Iron chelating activity (\%)} = \left[\frac{A_0 - A_s}{A_o}\right] \text{x } 100 \quad \textbf{(2)}$$

A_o is the absorbance of the blank (sample volume replaced by ultrapure water), and A_s is the absorbance of the sample (control/hydrolysates). The half-maximal effective concentration (EC_{50}) was determined as the hydrolysate concentration required for 50 % iron chelation activity.

2.5.1.3. ABTS radical scavenging activity

The ABTS radical scavenging activity was determined as previously reported.[21] 7 mM ABTS stock solution was prepared in phosphate buffer (4 mM, pH 7.4). The solution was maintained in total darkness at room temperature for 16 h before use. Then, an aliquot of the ABTS stock solution was diluted with the buffer to obtain an initial absorbance value of 0.70 ± 0.02 at 734 nm. 150 µL hydrolysate (0-0.4 mg/mL) or Trolox® (0-0.03 mg/mL used as positive control) were mixed with 150 µL ABTS radical, shaking for 10 s. After 10 minutes of incubation at 25 ºC, the absorbance of the reaction was measured at 734 nm. The ABTS radical scavenging activity was calculated with the **Equation 3**.

$$\text{ABTS radical scavenging (\%)} = \left[\frac{A_0 - A_s}{A_o}\right] \text{x } 100 \quad (3)$$

Where A_0 represents the initial absorbance of ABTS radical solution (sample volume replaced by buffer), and A_s indicates the absorbance of the remaining radical (with samples).

The EC_{50} was determined as hydrolysate/control concentration required for scavenging 50 % of ABTS radical. In addition, the TEAC index (Trolox® Equivalent Antioxidant Capacity) was determined from the calibration curve and results were expressed as µmol Trolox® equivalent per gram of sample (µmol TE/g sample).

2.5.1.4. Reducing power

The reducing power was measured as previously reported.[21] Hydrolysates (0-3 mg/mL) and positive control (ascorbic acid, 0-1 mg/mL) were prepared in phosphate buffer (0.2 M, pH 6.6). An aliquot of each former dilution (70 µL) was mixed with 35 µL of 1%(w/v) potassium ferricyanide solution and, incubated at 50 °C for 20 min. Then, 135 µL of distilled water, 33 µL of 10% (v/v) trichloroacetic acid solution and 27 µL of 0.1 (w/v) $FeCl_3$ were added. The reduction product, *i.e.,* ferrocyanide, was further stabilized with ferric ions in order to produce Prussian blue. The absorbance was determined at 700 nm after 10 min of incubation at 25 °C. The ability of hydrolysates to reduce Fe^{3+} was expressed in percentage (%) and calculated following **Equation 4**.

$$\text{Reducing capacity (\%)} = 100 - \left[\frac{A_0 - A_s}{A_o}\right] \text{x } 100 \quad \textbf{(4)}$$

Where A_o is absorbance of a 66 µM Prussian blue solution in the same reaction medium, and A_s is sample absorbance.

Results were expressed as effective concentration of hydrolysates able to reach 50 % the maximal reducing power capacity (EC_{50}).

2.5.2. IMAC experiments

The Cu^{2+}-chelating peptides present in whole and ≤ 1 kDa fractions of hydrolysates were fractionated by IMAC-Cu^{2+} using a HPLC system (LC-20AD, Shimadzu, Japan) at 1 mL/min flow rate, an oven temperature set at 25 ºC and a Diode Array Detector (SPD-M20A, Shimadzu, Japan). MCPs were separated on a 1 mL HisTrap^{TM}HP column (7 x 250 mm) prepacked with Ni Sepharose High Performance (Cytiva, Marlborough, MA, USA). Experiments were carried out according to Irankunda et al. with modifications.[22] The method included five steps described below in details: (i) Cu^{2+} regeneration (*i.e.,* Ni^{2+} ions were removed and replaced by Cu^{2+} ions), (ii) equilibration, (iii) injection followed by unbound compounds removal, (iv) elution, and (v) washing.

First, 10 column volumes (CV) of ultrapure water were used to remove the ethanol remaining in the column (storage conditions). Then, the column was stripped using 50 mM EDTA solution to remove Ni^{2+} immobilized ions, followed by Cu^{2+} regeneration step using 10 CV of a 0.1 M $CuSO_4.5H_2O$ solution. Then, 20 CV of equilibration buffer (PBS 1X pH 7.4: $Na_2HPO_4.12H_2O$ 6.7 mM; KH_2PO_4 1.25 mM; NaCl 300 mM) were used to remove the unbound copper ions and equilibrate the column. Finally, 50 µL of hydrolysates (20 mM eq NH_2 according to OPA assay) were loaded onto IMAC-Cu^{2+} column. The first fraction (F1) labeled non-copper-chelating peptides was eluted with the equilibration buffer after 5 min in order to remove peptides without metal-chelating properties, then the Cu^{2+}-chelating peptides (F2-F4) were eluted with an imidazole gradient (0-50 mM, prepared in PBS 1X pH 7.4) for 60 min. Finally, a 300 mM imidazole solution was used to wash the columns before the next run. The absorbance of the eluate was monitored at 280 nm. The F1-F4 fractions were collected using a fraction collector (FRC-10A, Shimadzu, Japan) for further LC-MS/MS identification analysis of Cu^{2+}-chelating peptides in hydrolysates. IMAC-Cu^{2+} experiments were performed in triplicate to ensure reproducibility. The retention time for each fraction (RT) was determined using the highest intensity point of the peak. This ensures consistency in identifying the elution profile of each sample. Retention times are reported as the mean of the three independent runs with their standard deviations.

2.5.3. Mass spectrometry identification and sequence analysis

LC-MS/MS analysis. To identify the peptide sequences present in the produced hydrolysates, the IMAC-Cu^{2+} collected fractions (F1-F4) were analysed on a Thermo Scientific UHPLC-HRMS system composed of a Vanquish™ liquid chromatography unit coupled to a photodiode array detector and an Orbitrap ID-X™ Tribrid™ high-resolution mass spectrometer operating in electrospray positive ionization mode (ESI^+) as previously reported.[23]

Peptide sequences identification. The Thermo Xcalibur raw LC-MS/MS data files resulting from the fractions (F1-F4) collected from the hydrolysates separated in IMAC- Cu^{2+} were processed in the Andromeda search engine of a commonly used proteomic software tools MaxQuant™ (version 2.4.13.0).[24] The peptides sequences were searched against a restricted sunflower seed proteins database (*Helianthus annuus*) containing 30 entries obtained from UniProtKB (https://www.uniprot.org/, accessed on 27 January 2024, Supplementary data, Table SD1). The parameters of database searches were set up as previously described (Table SD2).[24] Before searching peptides sequences from the collected fraction of hydrolysates, this method was first validated using a synthetic peptides hydrolysate, mixing 8 pure peptides at 1 mM each. These metal-chelating peptides (*i.e.*, AIPTGTA**H**, FATCIAR**H**, KFPILE**H**, KFPILE**H**L, KFPILE**H**LR, WL**H**NDGN, WL**H**NDGNTE, **W**VSFKTN) were obtained from 11S globulin seed storage protein G3 (P19084, 11S3_HELAN) present in sunflower seed. All the 8 peptides were identified (Supplementary data, Figure SD1). Finally, the AA composition of identified MCPs present in SMPI hydrolysates were computed through ExPASy ProtParam server (https://web.expasy.org/protparam/).

2.6. Statistical analysis

To evaluate the effect of enzymatic treatments and 1-kDa ultrafiltration process on physical-chemical and biofunctional properties of SMPI hydrolysates, results were statistically analyzed by one-way analysis of variance (ANOVA). All the measurements of OPA quantification and biofunctional properties (Cu^{2+}/Fe^{3+} ascorbate test, Fe^{2+}-chelating, radical scavenging, reduction power and Cu^{2+}-binding abilities) were obtained in quintuplicate and data presented as means ± standard deviation. In our study, we performed three replicates for each IMAC-Cu^{2+} experiment. Significant differences between means of samples were determined by Fisher's multiple range test. Differences at $p\text{-value} < 0.05$ were considered significant. Statistical calculations were conducted using the software Statgraphics centurion XVI version 16.1.03 (Statgraphics Technologies Inc, Virginia, USA).

3. Results and Discussion

3.1. Physicochemical characterization of the protein and hydrolysates

3.1.1. Protein content of sunflower meal protein isolate

The sunflower meal (SM) proteins were extracted using a NaCl extraction at pH 6, followed by isoelectric precipitation. The protein content initially present in SM (46.10 ± 0.9 %) increased up to 90.90 ± 2.7 % in SMPI, fulfilling the requirements of protein isolates (> 90 % of protein). Helianthinin *(i.e.,* 11S globulin) is the main storage protein in sunflower meal. The extractability of such protein increases by using NaCl, and upon the isoelectric precipitation at pH 4.5, the 11S globulin can be isolated, resulting in a protein content increase. SMPI obtained has a suitable protein content, and should be further considered as an alternative to obtain hydrolysates. Indeed, the SMPI produced in this study exhibits a similar protein content (90.90 ± 2.7 %) compared to that reported by Alexandrino et al.(92.08 %-98.6 %).[25]

The degree of hydrolysis (DH), defined as the percent of peptide bonds cleaved in a protein hydrolysate, is the first parameter used to characterize a hydrolysate. It provides primary information about the peptide size.[26] In our study, we were interested in small-sized peptides, commonly reported for their bioactivity. The DH parameter can only be measured for whole hydrolysate, i.e., before ultrafiltration.

Hydrolysates were prepared with Protamex® and Flavourzyme®, *i.e.,* complex mixtures of endo-peptidases and endo/exopeptidases, respectively. Due to their low cost, these enzymes are commonly used in the food industry to produce food-derived bioactive peptides. To enhance the hydrolysis of SMPI, a sequential enzymatic treatment was applied (Prot+Flav). After 2 h of hydrolysis, SMPI hydrolysates obtained using Protamex® or Flavourzyme® alone had a DH of 31 and 23 %, respectively (Table 1). This demonstrates that the endopeptidases contained in Protamex® can hydrolyze more SMPI compared with Flavourzyme®. As endopeptidase, Protamex® is an enzyme widely used in agro-industrial by-products hydrolysis, with an extensively broad specificity in peptide bond cleavage. Flavourzyme® cleaves peptide bonds between Leu and Pro or between two Pro residues.[27] Similar trend was reported in other studies, where the DH values of SMPI hydrolysates hydrolysed with Protamex® or Flavourzyme® alone were comprised within 10.37-20.05 %[4] and 5.93- 10.55 %[10], respectively.

Moreover, considering the specificity of each enzyme, the Flav treatment as endo/exopeptidases was carried out sequentially after the Prot treatment as endopeptidase only to improve the DH. The DH of Prot+Flav

hydrolysate increased up to 38 %, which was significantly higher than that of single enzymatic treatments. Thus, the number of N-terminal sites available for the activity of exopeptidases present in Flavourzyme® was increased by the first hydrolysis step with Protamex®.

Among the produced hydrolysates, Prot and Prot+Flav hydrolysates exhibit the highest DH values and were, therefore, selected for further analysis with their respective ≤ 1 kDa fractions.

Peptide quantification, as determined by OPA assay, refers to the measurement of free amino groups released during protein hydrolysis and it is expressed as mmol eq. NH_2/g of hydrolysate. This value is directly proportional to the concentration of peptides in the hydrolysate, since a higher production of peptides will result in a greater number of exposed amino groups. The peptide molar concentration increased from 0.39 to 0.89, 0.67 and 1.23 mmol eq. NH_2/g with hydrolysis of the SMPI by Prot, Flav, and Prot+Flav, respectively (Table 1). The peptide molar concentration notably increased in both ≤ 1 kDa fractions up to 1.16 and 3.33 for Prot and Prot+Flav, respectively. However, the most important difference was found in the sequential treatment, where Prot+Flav hydrolysate exhibits the highest amount of small-sized peptides.

3.1.2. Molecular weight distribution of peptides

3.1.2.1. SDS-PAGE

The MW distribution of protein constituents of the SM, SMPI and hydrolysates (Prot and Prot+Flav) was characterized by SDS-PAGE between 10-250 kDa (Figure 1A). First, the SM electrophoretic pattern shows four major, high-intensity band regions at approximately 35, 25, 20 and 10-15 kDa, corresponding to the 11S globulin subunits (α, α', β) and 2S albumins, respectively. The polypeptide composition of sunflower meal proteins presents a similar pattern to those reported in the literature.[3] Compared to sunflower meal (lane SM), notable changes in MW distribution of the protein isolate (lane SMPI) are observed, especially for the 2S albumins region. This band, representing residual 2S albumins, is of lower intensity due to the protein extraction process used, as 11S globulins are isolated from 2S albumins at their isoelectric point (pH 4.5).[18] Finally, the SDS-PAGE profile of Prot and Prot+Flav hydrolysates shows that the band intensity of 11S globulin subunits decreased, related to their partial Prot hydrolysis, producing peptides with MW range of 10-25 kDa (lane Prot). Finally, for the sequential treatment (lane Prot+Flav), bands with MW higher than 10 kDa disappeared while the bands corresponding to a high number of oligopeptides (<10 kDa) increased, due to the high proteolytic activity of exopeptidases in Flavourzyme®. These results are in line with those previously discussed for DH.

3.1.2.2. Size exclusion chromatography

The size exclusion chromatography (SEC) was used to estimate the MW of the hydrolysates (Prot and Prot+Flav) and their ≤ 1 kDa fractions (Figure 1B-C). Indeed, the peptides MW distribution plays a crucial role in their metal-chelating and antioxidant properties. The enzymatic treatments hydrolyzed the high MW protein of sunflower meal (above 20 kDa) into lower MW peptides (<10 kDa). The whole hydrolysates Prot and Prot+Flav exhibit the highest MW distribution in the range of > 3 kDa (45 %) and 0.2-0.6 kDa (64%), respectively. This finding can be explained by a higher production of small-sized peptides in Prot+Flav hydrolysate (DH: 38.80 %) compared to Prot one (DH: 30.96 %). Besides, in regard to the ≤ 1 kDa MWCO membrane ultrafiltration applied, the highest MW distribution was found from 0.2 to 0.6 kDa, with 76 and 86 % for ≤ 1 kDa Prot and ≤ 1 kDa Prot+Flav, respectively. Thus, it is possible to obtain protein hydrolysates from sunflower meal, enriched with small-sized peptides. Moreover, the SEC analysis is consistent with the DH and SDS-PAGE results. Our findings are in accordance with Sentís-Moré et al.[4], who reported a Protamex® sunflower hydrolysates, with MW distribution from 0.5 Da to 5 kDa. In contrast, Velliquette et al.[3] reported sunflower peptides with MW distribution ranging from 10 to 25 kDa after Flavourzyme® only.

In the present study, SM proteins were hydrolyzed using Protamex®, an enzyme that has previously been applied to this by-product. Previous work using Protamex® to hydrolyze SM protein focused primarily on the evaluation of physicochemical parameters (i.e., hydrolysis yield and molecular weight distribution), without reporting any information on the resulting bioactive properties. Besides, while the use of sequential enzymatic hydrolysis on SM protein has been investigated previously, to our knowledge the specific combination of Protamex® and Flavourzyme® used in our study has not been reported previously. Therefore, by evaluating the biofunctional characterization of these hydrolysates, this study allows to establish a relationship between enzymatic treatment, peptide composition and antioxidant mechanisms. This highlights our approach over previous studies and reinforces the potential of sunflower meal as a valuable source of MCPs.

3.2. Biofunctional characterization of MCPs in SMPI hydrolysates

3.2.1. Antioxidant activities

3.2.1.1. Inhibition of Cu^{2+}-induced ROS production

Ascorbate test was used to evaluate the effect of Cu^{2+}/Fe^{3+} complexation by MCPs present in hydrolysates on the inhibition of ROS production (*i.e.,* $O_2^{\bullet-}$, $HO^{\bullet}$) generated through Fenton-type reaction at physiological pH 7.4 (Figure 2A).[19, 20]

The ascorbate test results for the inhibition of Cu^{2+}-induced ROS production are presented for all the obtained hydrolysates and expressed as ascorbate consumed after 3 min (Figure 2B). The negative control (buffer) displays the highest ascorbate consumption, associated with its oxidation into dehydroascorbic acid, with a value of 46.5 µM, indicating the maximal ROS production. In the same test, the positive control, *i.e.,* EDTA, clearly showed the lowest ascorbate consumption, which is related with its strong Cu^{2+}-chelating ability. Compared to the negative control, all the whole and ≤ 1 kDa fraction samples significantly (*p-value* < 0.05) decreased the absorbate consumption. This indicates that, after Cu^{2+} complexation by peptides present in hydrolysates, Cu^{2+} was unable to catalyze the Fenton-type reaction to produce ROS in the redox cycle. The differences observed between hydrolysates can be attributed to the differences in peptide composition (peptide length, amino acid sequences). Interestingly, Prot hydrolysates (whole and ≤ 1 kDa fraction) present the most potent Cu^{2+}-chelating peptides. Copper-chelating ability could be associated with various amino acid residues such as His, Cys and Arg, as reported in sunflower protein[11, 28] and rice-bran-derived albumin hydrolysates.[29] Interestingly, the DH increase in the Prot+Flav sequential treatment does not enhance the Cu^{2+}-chelating ability, suggesting that Cu^{2+}-chelating sites of peptides have been destroyed upon sequential hydrolysis. Similar results were reported by Carrasco-Castilla et al. who produced lectin hydrolysates, whose Cu^{2+}-chelating ability decreased after extensive hydrolysis.[30] Yet, Peng et al. reported that Cu^{2+}-chelating ability of whey protein hydrolysates increased with increasing DH (from 19.3 to 38.5 %).[31] Moreover, small-sized peptides obtained after the 1 kDa MWCO ultrafiltration possessed a poor ROS inhibition associated with a lower Cu^{2+}-chelating ability (higher ascorbate consumed).

3.2.1.2. Inhibition of Fe^{3+}-induced ROS production

The inhibition of Fe^{3+}-induced ROS production of all hydrolysates expressed as ascorbate consumed after 10 min (Figure 2C) was different from the Cu^{2+}-induced ROS production. Here, EDTA, used as negative control

agent, showed the maximum ascorbate consumption (54 µM) while the ascorbate consumption decreased drastically to 3 µM (lowest value) for DFO, a positive control highly recognized as a Fe^{3+}-chelating agent. Regarding the hydrolysates, the ascorbate consumption decreased notably to the range 8-14 µM, suggesting that all the produced hydrolysates and their ≤ 1 kDa fractions contain Fe^{3+}-chelating peptides. The ability to complex Fe^{3+} to prevent ROS production is notably associated with the abundance of small-sized peptides in the hydrolysates. For instance, the whole Prot+Flav and both ≤ 1 kDa fractions hydrolysates, all characterized by their high peptide concentration expressed as mmol eq. NH_2/g of powder (OPA assay, Table 1, section 3.1.1) and correlated with their higher small-sized peptide (Figure 1C) compared to Prot hydrolysate, showed greater potential to prevent Fe^{3+}-induced ROS production than the whole Prot hydrolysate. Yet, this observed difference is only significant for the ≤ 1kDa Prot+ Flav hydrolysate. The Fe^{3+}-chelating ability is mostly influenced by factors such as MW, AA composition and their position within the sequence. Peptide sequences with abundance of negatively charged polar residues (Asp and Glu) can complex Fe^{3+} through carboxylate groups.[19] Additionally, the MW of peptides with Fe^{3+}-chelating ability usually ranges from 300-1500 Da, associated with a higher amount of carboxyl group available at each terminus of a peptide compared to larger-sized peptides.[32] Verma et al. reported a range of highest to lowest extent of Fe^{3+}-AA interaction as follows: Glu > Asp > His > Cys > Tyr > Gln > Lys > Asn > Ser > Trp, Leu, Arg, Ala.[32] These AA residues have been reported in the literature for sunflower meal and sunflower meal protein hydrolysate. [9,33] Based on our results, MCPs present in hydrolysates can complex Cu^{2+}/Fe^{3+} in solution, leading to the inhibition of metal-induced ROS generation.

3.2.1.3. Fe^{2+}-chelating activity

The ferrous state of iron (Fe^{2+}), one of the most important pro-oxidant agents, catalyzes ROS production through the Fenton reaction. Therefore, food-derived peptides endowed with iron-chelating properties may contribute to delay peroxidation and subsequently prevent cells and tissues damages.[34] The Fe^{2+}-chelating activity of the hydrolysates and their ≤ 1 kDa fractions was assessed by ferrozine test and expressed as EC_{50} (mg/mL) (Figure 3A-B). The lower the EC_{50} value, the higher the Fe^{2+}-chelating activity. For the whole hydrolysates, Prot hydrolysate showed higher Fe^{2+}-chelating activity than Prot+Flav ones. Indeed, the EC_{50} value increased significatively from 0.09 (Prot) to 0.82 mg/mL (Prot+Flav) after the sequential enzymatic treatment, meaning lower Fe^{2+}-chelating activity of the hydrolysate. Also, this suggests that sequential treatment using Flavourzyme® could hydrolyze a high number of MCPs peptides already produced by Prot. Regarding the two ≤ 1 kDa fractions, the same trend was found for both enzymatic treatments. Indeed, the

EC_{50} value of ≤ 1 kDa Prot+Flav could not be determined, as the activity was lower than 7 % in the range of concentration investigated (0-1 mg/mL). The Fe^{2+}-chelating activity was related with the presence of specific AA residues in the peptide sequence, such as negatively charged amino acids (Asp, Glu) and neutral polar amino acids (His, Cys).[32] Indeed, these AA were widely reported in sunflower meal and sunflower meal hydrolysates.[9, 33]

Our results demonstrate that the Fe^{2+}-chelating activity of hydrolysates is notably influenced by the MW distribution of peptides, where small-sized peptides (≤ 1 kDa) may not have enhanced this property. The high Fe^{2+}-chelating activity of Prot hydrolysate would be rather associated with the higher content of large-sized peptides than in Prot+Flav hydrolysate, where the enzymes can expose more efficient sites available for Fe^{2+}-chelation. Tang et al. found that the Fe^{2+}-chelating activity was affected negatively by significant decreases in peptide chain length due to extended hydrolysis in hemp (*Cannabis sativa L.*) protein isolate.[35] Similarly, in He et al. the whole hydrolysates and its 5-10 kDa fraction obtained from rapeseed protein exhibited the highest Fe^{2+}-chelating activity (lower EC_{50} values).[36]

In our study, Prot hydrolysates (whole and ≤ 1 kDa fraction) exhibited a stronger Fe^{2+}-chelating properties (lower EC_{50} values, EC_{50}: 0.09-0.10 mg/mL) compared to those reported in the literature for other hydrolysates from plant-derived proteins, including rapeseed protein (EC_{50} values > 3 mg/mL[36]), tree peony seed protein hydrolyzed by Alcalase, Neutrase and Papain enzymes (EC_{50}: 0.99-1.18 mg/mL[34]), mung bean protein (EC_{50}: 0.22-0.55 mg/mL[37]), and *Lentinus edodes* protein (EC_{50}: 0.99-2.7 mg/mL[27]). Taken together, our findings suggest that Prot hydrolysates from sunflower protein could be good metal-chelating agents to prevent the oxidative damages caused by ferrous ion in food and biological systems.

3.2.1.4. ABTS radical scavenging activity

The ability of hydrolysates to donate a hydrogen atom or an electron to scavenge free radicals was determined by measurement of ABTS radical scavenging activity (Figure 3C-D). All the hydrolysates exhibited dose-dependent ABTS radical scavenging activity from 0.02-0.4 mg/mL. The highest activity was reached at 0.4 mg/mL (> 87 %) (Figure 3C). With extended hydrolysis in Prot+Flav, a slight increase (*p-value* < 0.05) in EC_{50} value is observed, meaning a loss of ABTS radical scavenging activity (Figure 3D). Thus, during the sequential use of Flavourzyme®, some ABTS radical scavenging peptides produced in Prot may be cleaved further, leading to the decrease of this antioxidant property. Additionally, among the ≤ 1 kDa fractions, no significant

460 difference was observed (*p-value* > 0.05), suggesting that neither sequential treatment nor ≤ 1 kDa ultrafiltration
461 enhanced the ABTS radical scavenging activity.

462 The ABTS radical scavenging activity of hydrolysates could be attributed to peptides containing Phe, Tyr, Trp,
463 Cys and His, with their benzyl, phenolic, indoyl, sulfhydryl, and imidazole groups, respectively.[38] In our study,
464 the EC_{50} values of all the studied hydrolysates were lower (better activity) than those of peptides from
465 vegetable-derived proteins hydrolysed by Protamex® (tree peony seed protein, EC_{50}: 1.81 mg/mL[34] and mung
466 bean proteins, EC_{50}: 0.24 mg/mL).[37]

467 Furthermore, data were also reported as µM Trolox equivalent per gram of sample (µmol TE/g) to compare
468 our results with other studies (Figure 3D). In TEAC analysis, the higher the value, the higher the ABTS radical
469 scavenging activity. Overall, SMPI hydrolysates and their ≤ 1 kDa fractions scavenged the ABTS radical
470 effectively resulting in antioxidant activity. The TEAC value of Prot hydrolysate, which displays the highest
471 radical scavenging activity, is higher than those of peptides from hydrolysate of hemp seeds (124-240 µM
472 TE/g[39]), and similar to those of colocynth seeds (290-525 µM TE/g).[40] In contrast, higher values were reported
473 for canola proteins (5.45 mM TE/g).[41]

474 **3.2.1.5. Reducing power**

475 The ability of hydrolysates to reduce ferric ions (Fe^{3+}) into ferrous ions (Fe^{2+}) was evaluated using the
476 Fe^{3+}/ferricyanide assay, commonly used for measuring the antioxidant properties of food protein hydrolysates
477 in reference to ascorbic acid as positive control. The lower the EC_{50}, the higher the reducing power. All the
478 hydrolysates exhibited reducing power in a concentration-dependent manner (Figure 3E-F). Indeed, peptides
479 present in hydrolysates could present AA residues that act as an extra source of electrons and protons (Phe,
480 Try, Trp, Asp, and Gln).[34] Compared to Prot hydrolysates, the reducing power of Prot+Flav hydrolysates
481 increased markedly with increasing DH (lower EC_{50}, Figure 3F). Whatever the hydrolysate the hydrolysate,
482 the strongest reducing power was observed in ≤ 1 kDa Prot+Flav, related to its highest peptide concentration
483 (meaning smaller-sized peptides, **Table 1**). Similarly, the reducing power of several protein hydrolysates were
484 reported to increase when the number of small-sized peptides or the DH increased (tree peony seed protein[34];
485 mung bean protein[37]; sunflower meal).[42]

486 **3.2.2. Cu^{2+}-chelating peptides separation by IMAC**

487 The Cu^{2+}-chelating peptides present in the hydrolysates and their corresponding ≤ 1 kDa fractions were
488 separated/fractionated using IMAC-Cu^{2+}. This method, based on peptides-metal interaction, provides several

advantages due to its high-binding capacity and high recovery. The Cu^{2+}-chelating peptides were eluted using imidazole gradient. Yet, due to imidazole absorbing at 214 nm, which is also the wavelength used for monitoring peptide bonds, the peptides were followed at 280 nm. The IMAC-Cu^{2+}chromatogram shows the injection phase (0-5 min) and elution phase (5-65 min) of the hydrolysates (Figure 4A-D).

The imidazole gradient was applied (0-50 mM, 60 min, elution phase Figure 4) and Cu^{2+}-chelating peptides bound onto IMAC-Cu^{2+} phase were eluted in several peaks, *i.e.,* the fractions F2, F3, and even the fraction F4 for ≤ 1 kDa Prot+Flav only (Table 2). Among the hydrolysates, the retention time (RT) of the Cu^{2+}-chelating peptides fractions were not significantly different for F2 (RT: ~11 min) and F3 (RT: ~14 min) (*p-value* > 0.05). Thus, the mechanism of peptide-Cu^{2+} interaction in IMAC-Cu^{2+} column may be similar in the four hydrolysates and their difference in chelation capacity may rather be explained by the number of chelating peptides.

3.2.3. Identification of Cu^{2+}-chelating peptides by LC-MS/MS

The various fractions F1, F2, F3 and F4 were collected and subjected to LC-MS/MS analysis to identify the Cu^{2+}-chelating peptides sequences present in the hydrolysates. Figure 5A shows the total number of identified peptides in each fraction, with the highest number of Cu^{2+}-chelating peptides identified in Prot, followed by Prot+Flav and ≤ 1 kDa fractions. This observation strongly supports the high Cu^{2+}-chelating profile of Prot hydrolysate. The peptides sequences identified in the unbound peptides fraction F1 and in the enriched MCPs fractions F2-F3 are displayed in Table SD3 and Table 3, respectively. Interestingly, all the peptide sequences identified in F2 and F3 contain at least one His residue (Table 2), which plays a pivotal role in the Cu^{2+}-binding ability of hydrolysates due to its imidazole ring.[2] In comparison, His-containing peptides were not identified in the unbounding peptides fractions F1 (Table SD3). On the contrary, there may be other His-containing MCPs present in the F4 of ≤ 1 kDa Prot+Flav fraction, but they were not identified due to their low concentration compared to the whole hydrolysates and the sensitivity of analysis. Furthermore, the sequential treatment (Prot+Flav) does not show a better Cu^{2+}-chelating profile than the single treatment (Prot). Indeed, MS/MS analysis of F2 indicates that 7 new MCPs were generated in Prot+Flav after Flav treatment. However, 10 MCPs already present in Prot were hydrolysed, resulting in a lower total number (Prot+Flav: 12) of MCPs available to bind Cu^{2+} ions compared to Prot hydrolysate (Prot: 15) (Table 3).

To better understand the Cu^{2+}-chelating profile of the identified sequences, the AA composition of peptide sequences in F2 (fraction with the highest number of sequences) of all the hydrolysates were determined by

518 the free-accessed ProtParam tool (https://web.expasy.org/protparam/). In our study, we focused on
519 characterizing the AA composition of the metal-chelating peptide fraction itself (IMAC-Cu^{2+} fraction) rather
520 than the total AA composition of sunflower protein and its hydrolysate, already well-documented in the
521 literature. This AA analysis provides valuable insights into the functional properties of the peptides within this
522 specific fraction, allowing a deeper understanding of their metal chelating potential.
523 All the four hydrolysates contain His residue as the major amino acid in their sequences (>10 %), being the
524 main AA responsible for Cu^{2+}-binding properties of the hydrolysates (Figure 5B). In Prot hydrolysate, the
525 peptide sequences contain higher His content than the Prot+Flav hydrolysate, which could explain its high
526 Cu^{2+}-chelating properties (see Figure 2B inhibition of Cu^{2+}-induced ROS production). Negatively charged
527 (Asp and Glu) and positively charged amino acids (Arg and His) are the major potential metal-binding AA
528 residues present in the identified sequences (Figure 5B). Also, the peptide sequences contain high amount of
529 Glu, an important AA for Fe^{3+}-chelating properties, explaining the results of the inhibition of Fe^{3+}-induced
530 ROS production by the hydrolysates. Besides, Figure 5C reveals high amount of EAA, HAA, NCAA, and
531 PCAA in the identified MCPs, which have highly been associated with the antioxidant properties of food
532 protein hydrolysates.[38]
533 In comparison to the literature, several peptides identified from plant-derived proteins have been reported to
534 contain Histidine (His) residue (**Table 3**) as identified in our work. His-containing peptides are widely known
535 for their strong metal-chelating properties. Some examples include KP**H**K, EPS**H**, **H**ADAD, and
536 NAPLPPPLK**H**: these peptides identified from chia seed,[8] rapeseed,[6] mug bean[44] and wheat germ[14] protein
537 hydrolysates, respectively showed affinity for metal ions and potential bioactive properties. Similarly, MCPs
538 derived from agro-industrial by-product (e.g., SGSTG**H**, **H**LRQEEKEEVTVGSLK and FD**H**IVY) have also
539 been identified as bioactive peptides, which supports the potential of protein-rich waste materials for the
540 production of value-added functional peptides (**Table 3**).
541 More, another interesting comparison comes from the position of His within the peptide sequence. In our study,
542 His residues were mostly found in the first, second and third positions from the amino terminus (e.g.,
543 **H**NDGNTELVVVVF, P**H**YA and WV**H**NDGNAE) or in the first, second and third positions from
544 carboxylate terminus (e.g., GVDFIR**H**, DFIR**H**R, GTA**H**WL). Indeed, the different positions of His residue
545 in the structure of MCPs may define the stability of the formed peptide-Cu^{2+} complex.[47]. For instance, MCPs
546 with His residue in the first and third positions from the amino terminus could possess better stability in the
547 formed peptide-Cu^{2+} complex.[48] **Figure 6A-B** displays the sequenced mass spectra of two of the most

548 interesting sequences of Cu^{2+}-chelating peptides identified from SMPI hydrolysates loaded into MaxQuant
549 Viewer.
550 Product oxidation is one of the main challenges in the food industry. Metal ions such as Cu^{2+} and Fe^{2+} can lead
551 to lipid-rich food oxidation via Fenton and Haber-Weiss reaction. Oxidation reaction leads to color changes,
552 deterioration of nutritional properties, off-flavors up to texture changes. Due to their ability to bind these
553 transition metals, MCPs identified in our study could offer promising applications as food or pharmaceutical
554 bioactive agents to prevent metal-induced oxidation as previous work on inhibition of the lipid oxidation on
555 food emulsions by MCPs.[49] Finally, by valorising sunflower meal by-products to release MCPs, our approach
556 minimizes the waste and also promotes a circular economy model in the food and agricultural fields,
557 encouraging the development of high-value ingredients from renewable sources.
558 This study reported the physicochemical properties, metal-chelating and antioxidant activities of SMPI
559 hydrolysate obtained by single (Prot) and sequential (Prot+Flav) enzymatic treatments and their ≤ 1 kDa
560 fractions. For the first time, Cu^{2+}-chelating peptides were identified from SMPI hydrolysate using IMAC-Cu^{2+}
561 and their metal-chelating and metal-related antioxidant activities characterized. Upon sequential treatment,
562 large number of peptide bonds were cleaved effectively, releasing mainly small-sized peptides. Prot
563 hydrolysates contained higher number of larger-sized peptides compared to Prot+Flav. Some similarities were
564 observed between the Fe^{2+}-chelating, inhibition of Cu^{2+}-induced ROS production and ABTS radical
565 scavenging data. Indeed, the Prot hydrolysate and its corresponding ≤ 1 kDa fraction exhibited the highest
566 activities in these assays while the Prot+Flav and its ≤ 1 kDa fraction enhanced the Fe^{3+}-induced ROS and the
567 reducing power. Moreover, both MW distribution and AA residues of the sequences play a key role in metal-
568 chelating and antioxidant properties of peptides from SMPI. The molecular weight of Cu^{2+}-identified peptides
569 ranged from 0.8-1.7 kDa, with the larger-sized peptides (> 1 kDa) presenting the most effective bioactive
570 properties. Besides, the presence of His, Glu, Asp, and Arg in the peptide sequences identified improved the
571 metal-chelating and antioxidant properties. Taken together, sunflower meal by-product is an interesting protein
572 source to generate protein hydrolysates endowed with metal-chelating and antioxidant agents. According to
573 the structural characteristics of the sequences, the peptides identified in our study could serve as antioxidant
574 and MCPs candidates to be used as food or pharmaceutical active agents to prevent metal-induced oxidation
575 and diseases. Further works should deeply investigate the potential bioavailability of these MCPs in the context
576 of food applications including studies of gastrointestinal digestion and absorption.

Note that the pH, temperature and ionic strength variations may affect the stability and binding affinity of peptides to metals, since protonation or deprotonation of coordinating AA residues may modify the coordination properties and functionality. Therefore, future studies will be required to evaluate the stability of peptide-metal complexes over a range of pH and temperatures values and in the presence of physiologically relevant ions. These investigations would lead to a better understanding of the stability of the complexes under variable conditions, while also providing valuable insights for their practical application.

As future perspective, the use of molecular dynamic simulation and molecular docking of the peptide-Cu^{2+} complexes should be performed as theoretical approaches to gain a better insight into the interaction of peptides with metal ions prior to in vitro evaluation of peptides.

Abbreviations used:

AA, amino acids; AAA, aromatic amino acid; ABTS, 2,2′-azinobis (3-ethylbenzothiazoline-6-sulfonic acid) diammonium salt; ANOVA, one-way analysis of variance; $AscH^-$, ascorbate; BCAA, branched chain amino acids; CV, column volumes; DFO, deferoxamine; DH, degree of hydrolysis; EAA, essential amino acids; EC_{50}, half maximal effective concentration; EDTA, ethylenediaminetetraacetic acid; ESI^+, electrospray positive ionization mode; Flav, Flavourzyme®; HAA, hydrophobic amino acids; HPLC, high-performance liquid chromatography; IMAC, immobilized metal affinity chromatography; LC-MS/MS, liquid chromatography tandem mass spectrometry; MCPs, metal-chelating peptides; MW, molecular wight; MWCO, molecular weight cut-off; NCAA, negatively charged amino acids; OPA, *O*-phthaldialdehyde; PCAA, positively charged amino acids; PEG, polyethylene glycol; Prot, Protamex®; Prot+Flav, Protamex® followed by Flavourzyme®; ROS, reactive oxygen species; RT, retention time; SCAA, sulphur containing amino acids; SDS-PAGE, sodium dodecyl sulfate polyacrylamide gel electrophoresis; SEC, size exclusion chromatography; SM, sunflower meal by-product; SMPI, sunflower meal protein isolate; TCA, trichloroacetic acid; TEAC, Trolox® equivalent antioxidant capacity; Trolox®, 6-hydroxy-2,5,7,8-tetramethylchroman-2-carboxylic acid.

Author Contributions

J.A.C.E.: Conceptualization, Methodology, Data curation, Software, Formal analysis, Resources, Writing – original draft. C.M.: Methodology, Writing - review & editing. P.A.: Methodology, Data curation. C.P.: Methodology, Data curation, Writing - review & editing. L.S.: Methodology, Writing - review & editing. K.S.: Methodology, Writing - review & editing. C.C.U.: Methodology, Writing - review & editing. L.C-R.: Conceptualization, Project administration, Data curation, Formal analysis, Funding acquisition, Supervision, Visualization, Writing – review & editing.

Supporting information description

Protein data base used for peptide identification, parameters of database searches used for peptide identification, peptides sequences identified from sunflower meal protein hydrolysates, MaxQuant™ identification successfully carried out on a synthetic mixture containing 8 peptides at 1 mM.

Acknowledgments

The authors thank the French ministry government for the MESR grant, the ANR JCJC MELISSA (2020-2024), the "Impact Biomolecules" project of the "Lorraine Université d'Excellence"(Investissements d'avenir–ANR project number 15-004). The authors thank the PASM platform for the use of the Orbitrap LC-MS system (Plateau d'Analyse Structurale et Métabolomique - SF4242 EFABA, F-54505 Vandoeuvre-lès-Nancy, France).

4. References

(1) Li, Z.; Xiang, F.; Huang, X.; Liang, M.; Ma, S.; Gafurov, K.; Gu, F.; Guo, Q.; Wang, Q. Properties and Characterization of Sunflower Seeds from Different Varieties of Edible and Oil Sunflower Seeds. *Foods* **2024**, *13* (8), 1188. DOI: 10.3390/foods13081188.

(2) Camaño Echavarría, J. A.; El Hajj, S.; Irankunda, R.; Selmeczi, K.; Paris, C.; Udenigwe, C. C.; Canabady-Rochelle, L. L. S. Screening, Separation and Identification of Metal-Chelating Peptides for Nutrition, Cosmetic and Pharmaceutical Applications. *Food & Function* **2024**, *15* (15), 3300-3326. DOI: 10.1039/d3fo05765h.

(3) Velliquette, R. A.; Fast, D. J.; Maly, E. R.; Alashi, A. M.; Aluko, R. E. Enzymatically derived sunflower protein hydrolysate and peptides inhibit NFkappaB and promote monocyte differentiation to a dendritic cell phenotype. *Food Chem* **2020**, *319*, 126563. DOI: 10.1016/j.foodchem.2020.126563.

(4) Sentís-Moré, P.; Ortega-Olivé, N.; Mas-Capdevila, A.; Romero-Fabregat, M.-P. Impact of centrifugation and vacuum filtration step on the yield and molecular weight distribution of protein hydrolysates from rapeseed and sunflower meals. *Lwt* **2022**, *165*. DOI: 10.1016/j.lwt.2022.113741.

(5) Tonolo, F.; Coletta, S.; Fiorese, F.; Grinzato, A.; Albanesi, M.; Folda, A.; Ferro, S.; De Mario, A.; Piazza, I.; Mammucari, C.; et al. Sunflower seed-derived bioactive peptides show antioxidant and anti-inflammatory activity: From in silico simulation to the animal model. *Food Chem* **2024**, *439*, 138124. DOI: 10.1016/j.foodchem.2023.138124.

(6) Xie, N.; Huang, J.; Li, B.; Cheng, J.; Wang, Z.; Yin, J.; Yan, X. Affinity purification and characterisation of zinc chelating peptides from rapeseed protein hydrolysates: possible contribution of characteristic amino acid residues. *Food Chem* **2015**, *173*, 210-217. DOI: 10.1016/j.foodchem.2014.10.030.

(7) Lv, Y.; Wei, K.; Meng, X.; Huang, Y.; Zhang, T.; Li, Z. Separation and identification of iron-chelating peptides from defatted walnut flake by nanoLC-ESI–MS/MS and de novo sequencing. *Process Biochem* **2017**, *59*, 223-228. DOI: 10.1016/j.procbio.2017.05.010.

(8) Latha, B. V.; Likhitha, R.; Kumar, M. Copper chelating protein hydrolysate from Salvia hispanica L. by pepsin-pancreatin treatment. *Curr Res Food Sci* **2021**, *4*, 829-839. DOI: 10.1016/j.crfs.2021.11.007.

(9) Dabbour, M.; He, R.; Mintah, B.; Ma, H. Antioxidant activities of sunflower protein hydrolysates treated with dual-frequency ultrasonic: Optimization study. *Journal of Food Process Engineering* **2019**, *42* (5). DOI: 10.1111/jfpe.13084.

(10) Bao, X.; Yuan, X.; Feng, G.; Zhang, M.; Ma, S. Structural characterization of calcium-binding sunflower seed and peanut peptides and enhanced calcium transport by calcium complexes in Caco-2 cells. *J Sci Food Agric* **2021**, *101* (2), 794-804. DOI: 10.1002/jsfa.10800.

(11) Megías, C.; Pedroche, J.; Yust, M. M.; Girón-Calle, J.; Alaiz, M.; Millán, F.; Vioque, J. Production of copper-chelating peptides after hydrolysis of sunflower proteins with pepsin and pancreatin. *LWT* **2008**, *41* (10), 1973-1977. DOI: 10.1016/j.lwt.2007.11.010.

(12) Guo, L.; Harnedy, P. A.; O'Keeffe, M. B.; Zhang, L.; Li, B.; Hou, H.; FitzGerald, R. J. Fractionation and identification of Alaska pollock skin collagen-derived mineral chelating peptides. *Food Chem* **2015**, *173*, 536-542. DOI: 10.1016/j.foodchem.2014.10.055.

(13) Canabady-Rochelle, L. L. S.; Selmeczi, K.; Collin, S.; Pasc, A.; Muhr, L.; Boschi-Muller, S. SPR screening of metal chelating peptides in a hydrolysate for their antioxidant properties. *Food Chem* **2018**, *239*, 478-485. DOI: 10.1016/j.foodchem.2017.06.116.

(14) Zhu, K.-X.; Wang, X.-P.; Guo, X.-N. Isolation and characterization of zinc-chelating peptides from wheat germ protein hydrolysates. *J. Funct. Foods* **2015**, *12*, 23-32. DOI: 10.1016/j.jff.2014.10.030.

(15) Kalpana, B.; Ramya, K.; Munishamanna, K.; Palanimuthu, V. Extraction of protein from sunflower Deoiled cake. *Journal of Pharmacognosy and Phytochemistry* **2020**, *9* (3), 3-27.

(16) El Hajj, S.; Irankunda, R.; Camano Echavarria, J. A.; Arnoux, P.; Paris, C.; Stefan, L.; Gaucher, C.; Boschi-Muller, S.; Canabady-Rochelle, L. Metal-chelating activity of soy and pea protein hydrolysates obtained after different enzymatic treatments from protein isolates. *Food Chem* **2023**, *405* (Pt A), 134788. DOI: 10.1016/j.foodchem.2022.134788.

(17) Camaño Echavarría, J. A.; Irankunda, R.; Arnoux, P.; Mathé, C.; Girardet, J.-M.; Cakir-Kiefer, C.; Risler, A.; Stefan, L.; Paris, C.; Zapata Montoya, J. E.; et al. Characterization and Bioactivities of Gelatin Hydrolysates of Red Tilapia (Oreochromis spp.) Scale Byproducts. *ACS Food Science & Technology* **2025**. DOI: 10.1021/acsfoodscitech.4c00918.
(18) Zilic, S.; Barac, M.; Pesic, M.; Crevar, M.; Stanojevic, S.; Nisavic, A.; Saratlic, G.; Tolimir, M. Characterization of sunflower seed and kernel proteins. *Helia* **2010**, *33* (52), 103-113. DOI: 10.2298/hel1052103z.
(19) Csire, G.; Dupire, F.; Canabady-Rochelle, L.; Selmeczi, K.; Stefan, L. Bio-Inspired Casein-Derived Antioxidant Peptides Exhibiting a Dual Direct/Indirect Mode of Action. *Inorg Chem* **2022**, *61* (4), 1941-1948. DOI: 10.1021/acs.inorgchem.1c03085.
(20) Pradhan, K.; Das, G.; Kar, C.; Mukherjee, N.; Khan, J.; Mahata, T.; Barman, S.; Ghosh, S. Rhodamine-Based Metal Chelator: A Potent Inhibitor of Metal-Catalyzed Amyloid Toxicity. *ACS Omega* **2020**, *5* (30), 18958-18967. DOI: 10.1021/acsomega.0c02235.
(21) Canabady-Rochelle, L. L.; Harscoat-Schiavo, C.; Kessler, V.; Aymes, A.; Fournier, F.; Girardet, J. M. Determination of reducing power and metal chelating ability of antioxidant peptides: revisited methods. *Food Chem* **2015**, *183*, 129-135. DOI: 10.1016/j.foodchem.2015.02.147.
(22) Irankunda, R.; Camaño Echavarría, J. A.; Paris, C.; Selmeczi, K.; Stefan, L.; Boschi-Muller, S.; Muhr, L.; Canabady-Rochelle, L. Deciphering Interactions Involved in Immobilized Metal Ion Affinity Chromatography and Surface Plasmon Resonance for Validating the Analogy between Both Technologies. *Inorganics* **2024**, *12* (1), 31. DOI: 10.3390/inorganics12010031.
(23) Dos Santos Morais, R.; El-Kirat-Chatel, S.; Burgain, J.; Simard, B.; Barrau, S.; Paris, C.; Borges, F.; Gaiani, C. A Fast, Efficient and Easy to Implement Method to Purify Bacterial Pili From Lacticaseibacillus rhamnosus GG Based on Multimodal Chromatography. *Front Microbiol* **2020**, *11*, 609880. DOI: 10.3389/fmicb.2020.609880.
(24) Boachie, R. T.; Okagu, O. D.; Abioye, R.; Huttmann, N.; Oliviero, T.; Capuano, E.; Fogliano, V.; Udenigwe, C. C. Lentil Protein and Tannic Acid Interaction Limits in Vitro Peptic Hydrolysis and Alters Peptidomic Profiles of the Proteins. *J Agric Food Chem* **2022**, *70* (21), 6519-6529. DOI: 10.1021/acs.jafc.2c00197.
(25) Alexandrino, T. D.; Ferrari, R. A.; de Oliveira, L. M.; de Cássia S.C. Ormenese, R.; Pacheco, M. T. B. Fractioning of the sunflower flour components: Physical, chemical and nutritional evaluation of the fractions. *Lwt* **2017**, *84*, 426-432. DOI: 10.1016/j.lwt.2017.05.062.
(26) Nielsen, P. M.; Petersen, D.; Dambmann, C. Improved Method for Determining Food Protein Degree of Hydrolysis. *Journal of Food Science* **2001**, *66* (5), 642-646. DOI: 10.1111/j.1365-2621.2001.tb04614.x.
(27) Bing, S. J.; Chen, X. S.; Zhong, X.; Li, Y. Q.; Sun, G. J.; Wang, C. Y.; Liang, Y.; Zhao, X. Z.; Hua, D. L.; Chen, L.; et al. Structural, functional and antioxidant properties of Lentinus edodes protein hydrolysates prepared by five enzymes. *Food Chem* **2024**, *437* (Pt 1), 137805. DOI: 10.1016/j.foodchem.2023.137805.
(28) Megías, C.; Pedroche, J.; Yust, M. M.; Girón-Calle, J.; Alaiz, M.; Millán, F.; Vioque, J. Affinity Purification of Copper-Chelating Peptides from Sunflower Protein Hydrolysates. *J. Agric. Food Chem* **2007**, *55*, 6509-6514.
(29) Kubglomsong, S.; Theerakulkait, C.; Reed, R. L.; Yang, L.; Maier, C. S.; Stevens, J. F. Isolation and Identification of Tyrosinase-Inhibitory and Copper-Chelating Peptides from Hydrolyzed Rice-Bran-Derived Albumin. *J Agric Food Chem* **2018**, *66* (31), 8346-8354. DOI: 10.1021/acs.jafc.8b01849.
(30) Carrasco-Castilla, J.; Hernández-Álvarez, A. J.; Jiménez-Martínez, C.; Jacinto-Hernández, C.; Alaiz, M.; Girón-Calle, J.; Vioque, J.; Dávila-Ortiz, G. Antioxidant and metal chelating activities of Phaseolus vulgaris L. var. Jamapa protein isolates, phaseolin and lectin hydrolysates. *Food Chem* **2012**, *131* (4), 1157-1164. DOI: 10.1016/j.foodchem.2011.09.084.
(31) Peng, X.; Kong, B.; Xia, X.; Liu, Q. Reducing and radical-scavenging activities of whey protein hydrolysates prepared with Alcalase. *International Dairy Journal* **2010**, *20* (5), 360-365. DOI: 10.1016/j.idairyj.2009.11.019.
(32) Verma, S. K.; Sharma, A.; Sandhu, P.; Choudhary, N.; Sharma, S.; Acharya, V.; Akhter, Y. Proteome scale identification, classification and structural analysis of iron-binding proteins in bread wheat. *J Inorg Biochem* **2017**, *170*, 63-74. DOI: 10.1016/j.jinorgbio.2017.02.012.

(33) Ugolini, L.; Cinti, S.; Righetti, L.; Stefan, A.; Matteo, R.; D'Avino, L.; Lazzeri, L. Production of an enzymatic protein hydrolyzate from defatted sunflower seed meal for potential application as a plant biostimulant. *Industrial Crops and Products* **2015**, *75*, 15-23. DOI: 10.1016/j.indcrop.2014.11.026.
(34) Wang, Y. Y.; Wang, C. Y.; Wang, S. T.; Li, Y. Q.; Mo, H. Z.; He, J. X. Physicochemical properties and antioxidant activities of tree peony (Paeonia suffruticosa Andr.) seed protein hydrolysates obtained with different proteases. *Food Chem* **2021**, *345*, 128765. DOI: 10.1016/j.foodchem.2020.128765.
(35) Tang, C.-H.; Wang, X.-S.; Yang, X.-Q. Enzymatic hydrolysis of hemp (Cannabis sativa L.) protein isolate by various proteases and antioxidant properties of the resulting hydrolysates. *Food Chemistry* **2009**, *114* (4), 1484-1490. DOI: 10.1016/j.foodchem.2008.11.049.
(36) He, R.; Girgih, A. T.; Malomo, S. A.; Ju, X.; Aluko, R. E. Antioxidant activities of enzymatic rapeseed protein hydrolysates and the membrane ultrafiltration fractions. *Journal of Functional Foods* **2013**, *5* (1), 219-227. DOI: 10.1016/j.jff.2012.10.008.
(37) Liu, F. F.; Li, Y. Q.; Wang, C. Y.; Liang, Y.; Zhao, X. Z.; He, J. X.; Mo, H. Z. Physicochemical, functional and antioxidant properties of mung bean protein enzymatic hydrolysates. *Food Chem* **2022**, *393*, 133397. DOI: 10.1016/j.foodchem.2022.133397.
(38) Wen, C.; Zhang, J.; Zhang, H.; Duan, Y.; Ma, H. Plant protein-derived antioxidant peptides: Isolation, identification, mechanism of action and application in food systems: A review. *Trends Food Sci Technol* **2020**, *105*, 308-322. DOI: 10.1016/j.tifs.2020.09.019.
(39) Yoon, H.-J.; Park, G.-H.; Lee, Y.-R.; Lee, J.-M.; Ahn, H.-L.; Lee, S.-O. Enzymatic preparation and antioxidant activities of protein hydrolysates from hemp (Cannabis sativa L.)seeds. *Korean Journal of Food Preservation* **2023**, *30* (3), 434-445. DOI: 10.11002/kjfp.2023.30.3.434.

(40) Alblooshi, M.; Devarajan, A. R.; Singh, B. P.; Ramakrishnan, P.; Mostafa, H.; Kamal, H.; Mudgil, P.; Maqsood, S. Multifunctional bioactive properties of hydrolysates from colocynth (Citrullus colocynthis) seeds derived proteins: Characterization and biological properties. *Plant Physiol Biochem* **2023**, *194*, 326-334. DOI: 10.1016/j.plaphy.2022.11.026.

(41) Bermejo-Cruz, M.; Osorio-Ruiz, A.; Rodríguez-Canto, W.; Betancur-Ancona, D.; Martínez-Ayala, A.; Chel-Guerrero, L. Antioxidant potential of protein hydrolysates from canola (Brassica napus L.) seeds. *Biocatalysis and Agricultural Biotechnology* **2023**, *50*. DOI: 10.1016/j.bcab.2023.102687.
(42) Dabbour, M.; Hamoda, A.; Wahia, H.; Mintah, B. K.; Betchem, G.; He, R.; Ma, H.; Fikry, M. Functional, conformational, topographical, and antioxidative properties of convectively- and freeze-dried sunflower protein and hydrolysate: a comparative investigation. *Drying Technology* **2023**, *41* (12), 1962-1976. DOI: 10.1080/07373937.2023.2209805.
(43) Bao, X.; Ma, S.; Fu, Y.; Wu, J.; Zhang, M. Sensory and structural characterization of umami peptides derived from sunflower seed. *CyTA - Journal of Food* **2020**, *18* (1), 485-492. DOI: 10.1080/19476337.2020.1778794.
(44) Budseekoad, S.; Yupanqui, C. T.; Sirinupong, N.; Alashi, A. M.; Aluko, R. E.; Youravong, W. Structural and functional characterization of calcium and iron-binding peptides from mung bean protein hydrolysate. *J. Funct. Foods* **2018**, *49*, 333-341. DOI: 10.1016/j.jff.2018.07.041.
(45) Chen, D.; Liu, Z.; Huang, W.; Zhao, Y.; Dong, S.; Zeng, M. Purification and characterisation of a zinc-binding peptide from oyster protein hydrolysate. *J. Funct. Foods* **2013**, *5* (2), 689-697. DOI: 10.1016/j.jff.2013.01.012.
(46) Liao, W.; Chen, H.; Jin, W.; Yang, Z.; Cao, Y.; Miao, J. Three Newly Isolated Calcium-Chelating Peptides from Tilapia Bone Collagen Hydrolysate Enhance Calcium Absorption Activity in Intestinal Caco-2 Cells. *J Agric Food Chem* **2020**, *68* (7), 2091-2098. DOI: 10.1021/acs.jafc.9b07602.
(47) Sóvágó, I.; Kállay, C.; Várnagy, K. Peptides as complexing agents: Factors influencing the structure and thermodynamic stability of peptide complexes. *Coordination Chemistry Reviews* **2012**, *256* (19-20), 2225-2233. DOI: 10.1016/j.ccr.2012.02.026.
(48) Camaño Echavarria, J. A.; Mathe, C.; Girardet, J. M.; Paris, C.; Udenigwe, C. C.; Selmeczi, K.; Canabady-Rochelle, L. Identification of Ni(2+)-binding peptides in sunflower meal protein

hydrolysate for deeper understanding of peptide-metal interactions. *J Inorg Biochem* **2025**, *269*, 112877. DOI: 10.1016/j.jinorgbio.2025.112877.
(49) Irankunda, R.; Bjorlie, M.; Yesiltas, B.; Muhr, L.; Canabady-Rochelle, L.; Jacobsen, C. Evaluation of primary and secondary oxidation products in fish oil-in-water emulsions: Effect of metal-complexing peptides and protein hydrolysates. *Food Chem* **2024**, *439*, 138042. DOI: 10.1016/j.foodchem.2023.138042.

Tables

Table 1. The degree of hydrolysis (DH) and peptide concentration of hydrolysates prepared by different enzymatic treatments determined by OPA assay. The DH can be measured only before ultrafiltration.

Samples	Degree of hydrolysis (%)	Peptide concentration* (mmol eq. NH_2/g)
SMPI	--	0.39 ± 0.11^{a}
Prot	30.96 ± 1.34^{a}	0.89 ± 0.04^{b}
Flav	23.33 ± 1.69^{b}	0.67 ± 0.04^{c}
Prot+Flav	38.80 ± 0.87^{c}	1.23 ± 0.02^{d}
≤ 1 kDa Prot	--	1.16 ± 0.03^{b}
≤ 1 kDa Prot + Flav	--	3.33 ± 0.01^{e}

*Peptide quantification refers to the measurement of free amino groups released during proteolysis as an indicator of peptide production. Higher values correspond to increased peptide concentrations, reflecting a higher degree of protein hydrolysis. Different letters indicate in the same column indicate the significant difference between the hydrolysates and their ≤ 1 kDa fractions (*p-value* < 0.05). n=5. DH: degree of hydrolysis; Prot: Protamex® hydrolysate; Prot+Flav: Protamex® followed by Flavourzyme® hydrolysate; ≤ 1 kDa: 1 kDa ultrafiltrated hydrolysate.

852 **Table 2.** Reproducibility of IMAC-Cu^{2+} separation experiments: Retention times (mean ± standard deviation)
853 of peptide fractions obtained from sunflower meal protein hydrolysates.

Sample	Retention time of a given fraction (min)			
	F1	F2	F3	F4
Prot	1.28 ± 0.1[a]	10.9 ± 0.3[a]	14.65 ± 0.2[a]	NO
Prot+Flav	1.41 ± 0.3[a]	10.8 ± 0.3[a]	14.20 ± 0.4[a]	NO
≤ 1 kDa Prot	1.21 ± 0.1[a]	10.7 ± 0.2[a]	14.1 ± 0.3[a]	NO
≤ 1 kDa Prot+Flav	1.24 ± 0.2[a]	10.8 ± 0.2[a]	14.5 ± 0.4[a]	20.9 ± 0.5

854 Different letters in the same column indicate the significant difference between the hydrolysates and their ≤ 1 kDa
855 fractions (*p-value* < 0.05). n=3. F1: fraction collected before the elution gradient (0–5 min in the chromatogram),
856 containing unbound peptides with no affinity for Cu^{2+} ions; F2: first fraction of Cu^{2+}-bound peptides eluted using
857 imidazole; F3: second fraction of Cu^{2+}-bound peptides obtained upon further elution with imidazole, F4: third fraction of
858 Cu^{2+}-bound peptides, observed only in the ≤ 1 kDa Prot+Flav hydrolysate, collected after additional imidazole elution.
859 Prot: Protamex® hydrolysate; Prot+Flav: Protamex® followed by Flavourzyme® hydrolysate; ≤ 1 kDa: 1 kDa ultrafiltrated
860 hydrolysate; NO: not observed.
861
862
863
864
865
866
867
868
869
870
871
872
873
874
875
876
877
878
879
880
881
882
883
884

885 **Table 3.** Cu^{2+}-chelating peptides identified from the F2-F3 sunflower meal protein isolate hydrolysates
886 fractions using IMAC-Cu^{2+} separation followed by LC-MS/MS analysis.

887

Sequence	Intensity (x 10^4)				Length	Mass (g/mol)	Score	Entry
	Prot	Prot+Flav	≤ 1 k Da Prot	≤ 1 kDa Prot+Flav				
Fraction 2 (RT ≈ 11 min)								
AGGISSE**H**IQGQQQ	NI	1553.80	NI	NI	14	1438.68	12.87	A0A251UYX1
AIQSP**H**	61.49	NI	30.21	NI	6	651.33	4.66	P19084
AVLAP**H**	49.70	NI	26.83	NI	6	606.35	1.42	A0A251T566
DFIR**H**	432.36	165.68	231.62	NI	5	686.35	10.80	A0A251TKL9
FPILE**H**	NI	37.99	NI	72.46	6	754.40	1.42	P19084
FPILE**H**L	NI	253.26	NI	124.96	7	867.49	3.24	P19084
FSP**H**	163.85	NI	103.38	NI	4	486.22	8.08	A0A251UYX1
FVTPEEEQQQM**H**	76.69	NI	NI	NI	12	1501.65	1.19	
GENDQRG**H**IIF	36.28	507.19	NI	NI	11	1284.62	0.51	A0A251TUS1
GENDQRG**H**IIFVQ	NI	130.80	NI	NI	13	1511.75	1.52	
GISSE**H**IQGQ	NI	NI	NI	21.07	10	1054.50	0.46	A0A251UYX1
GIVSP**H**	93.97	NI	58.57	12.87	6	608.33	4.66	A0A251TUS1
GVDFIR**H**	252.44	78.13	118.11	79.36	7	842.44	12.16	A0A251TKL9
HNDGNTELVVVVF	NI	239.82	NI	NI	13	1441.72	4.72	
HVDQETASKL	94.04	NI	NI	NI	10	1126.56	1.84	A0A9K3HVJ0
NIDNPS**H**ADFVNPQ	216.29	NI	NI	NI	14	1566.71	1.74	A0A9K3NGE6
P**H**YA	99.76	NI	NI	NI	4	486.22	2.71	A0A9K3JEW0
RGENDQRG**H**IIF	674.32	NI	NI	NI	12	1440.72	2.73	A0A251TUS1
SEVF**H**	NI	NI	NI	45.03	5	617.28	1.94	A0A9K3HVJ0
SEVF**H**VD	161.31	155.86	NI	NI	7	831.38	3.24	
SFLAGGISSE**H**IQGQQQ		395.13	NI	NI	17	1785.86	2.25	A0A251UYX1
SP**H**WTIN	25.57	121.55	28.07	49.29	7	853.41	11.11	P19084
WV**H**NDGNAE	21.03	NI	NI	NI	9	1040.43	0.52	A0A9K3NGE6
YANQLDPN**H**RRF	NI	54.97	NI	NI	12	1529.75	1.19	A0A251TUS1
Fraction 3 (RT ≈ 14 min)								
ALFSP**H**	304.06	NI	72.077	NI	6	670.34	14.67	A0A251UYX1
DFIR**H**R	151.10	NI	45.85	6.16	6	842.45	4.12	A0A251TKL9
GTA**H**WL	60.17	NI	NI	NI	6	683.34	1.42	P19084
GVDFIR**H**R	484.99	22.71	161.79	24.31	8	998.54	3.60	A0A251TKL9
NPS**H**ADFV	NI	NI	NI	16.08	8	885.40	0.60	A0A9K3NGE6
Metal-chelating peptides previously reported in hydrolysates from plant-derived proteins or from byproducts								
EFEGGSIE**H**	Sunflower seed hydrolysate[43]				9	1004.01	NR	Putative 11-S
KP**H**K	Chia seed protein hydrolysate[8]				4	508.61	NR	NR
EPS**H**	Rapeseed protein hydrolysate[6]				4	468.47	NR	Cruciferin precursor
HADAD	Mug bean protein hydrolysate[44]				5	527.49	NR	NR
NAPLPPPLK**H**	Wheat germ hydrolysate[14]				10	1083.28	NR	NR
SGSTG**H**	Fish skin gelatin hydrolysate[12]				6	545.24	NR	Collagen a3(I)
HLRQEEKEEVTVGSLK	Oyster protein hydrolysate[45]				16	1882.08	NR	NR
FD**H**IVY	Tilapia bone hydrolysate[46]				6	793.38	NR	I3IYK1

888 Prot: Protamex® hydrolysate; Prot+Flav: Protamex® followed by Flavourzyme® hydrolysate; ≤ 1 kDa: 1 kDa ultrafiltrated
889 hydrolysate; NI: not identified; NR: not reported. F2: first fraction of Cu^{2+}-bound peptides eluted using imidazole; F3:
890 second fraction of Cu^{2+}-bound peptides obtained upon further elution with imidazole.

Figures captions

Fig. 1. Molecular weight distribution of protein and peptides hydrolysates from SMPI. (A) SDS-PAGE profile (12.5 %) of sunflower meal, sunflower meal protein isolate, and whole protein hydrolysates (Prot and Pro). (B) and (C) size exclusion chromatographic profile of sunflower meal protein isolate hydrolysates and their ≤ 1 kDa fractions. M: Marker; SM: sunflower meal; SMPI: sunflower meal protein isolate; Prot: Protamex® hydrolysate; Prot+Flav: Protamex® followed by Flavourzyme® hydrolysate; ≤ 1 kDa: 1 kDa ultrafiltrated hydrolysate; PEG: Polyethylene glycol.

Fig. 2. (A) The process for generating reactive oxygen species (ROS) *via* the Fenton reaction cycle involves molecular oxygen and ascorbate in the presence of copper and iron ions. (B-C) The inhibition of Cu^{2+}/Fe^{3+}-induced ROS production by chelating copper assessed by measuring ascorbate absorbance intensity at 265 nm. Error bar corresponds to the standard deviation. Different letters indicate the significant difference between samples (*p-value* < 0.05). n=3. $AscH^-$: ascorbate; DFO: deferoxamine; Prot: Protamex® hydrolysate; Prot+Flav: Protamex® followed by Flavourzyme® hydrolysate; ≤ 1 kDa: 1 kDa ultrafiltrated hydrolysate.

Fig. 3. Antioxidant activities of Prot, Prot+Flav, ≤ 1 kDa Prot and ≤ 1 kDa Prot+Flav hydrolysates. Fe^{2+}-chelating activity (A), ABTS radical scavenging activity (C), and reducing power ability (E) as a function of hydrolysate concentration. Half efficient concentration EC_{50} (mg/mL) values determined for Fe^{2+}-chelating (B), ABTS radical scavenging (D), and reducing power activities (F). Error bar corresponds to the standard deviation. Different letters indicate significant difference between samples (*p-value* < 0.05). n=5. TEAC: Trolox equivalent antioxidant capacity; Prot: Protamex® hydrolysate; Prot+Flav: Protamex® followed by Flavourzyme® hydrolysate; ≤ 1 kDa Prot: Protamex® hydrolysate; Prot+Flav: Protamex® followed by Flavourzyme® hydrolysate; ≤ 1 kDa: 1 kDa ultrafiltrated hydrolysate.

Fig. 4. The fractionation of Cu^{2+}-chelating peptides of sunflower meal protein isolate hydrolysates obtained by different enzymatic treatments. The unbounding (injection phase) and bound peptides (elution phase) present in Prot (A), Prot+Flav (B), ≤ 1 kDa Prot (C) and ≤ 1 kDa Prot+Flav (D). Prot: Protamex® hydrolysate; Prot+Flav: Protamex® followed by Flavourzyme® hydrolysate; ≤ 1 kDa Prot: Protamex® hydrolysate; Prot+Flav: Protamex® followed by Flavourzyme® hydrolysate; ≤ 1 kDa: 1 kDa ultrafiltrated hydrolysate.

Fig. 5. Results obtained from the MS/MS identification of peptides present in sunflower meal protein isolate hydrolysates. (A) Number of peptides identified in F1, F2 and F3 fraction in whole and ≤ 1 kDa fraction hydrolysates. (B) and (C) amino acid composition of Cu^{2+}-chelating peptides identified in the F2 fractions of all the hydrolysates. Prot: Protamex® hydrolysate; Prot+Flav: Protamex® followed by Flavourzyme® hydrolysate; ≤ 1 kDa Prot: Protamex® hydrolysate; Prot+Flav: Protamex® followed by Flavourzyme® hydrolysate; ≤ 1 kDa: 1 kDa ultrafiltrated hydrolysate. AAA: Aromatic amino acids= phenylalanine, tryptophan, tyrosine; NCAA: Negatively charged amino acids= aspartic acid, glutamic acid, asparagine, glutamine; PCAA: Positively charged amino acids= arginine, histidine, lysine; HAA: Total Hydrophobic amino acids= alanine, valine, isoleucine, leucine, tyrosine, phenylalanine, tryptophan, proline, methionine and cysteine; SCAA: Sulphur containing amino acids= methionine and cysteine; EAA: Essential amino acids= tryptophan, lysine, histidine, phenylamine, leucine, isoleucine, methionine, valine, threonine; BCAA: Branch chain amino acids= isoleucine; leucine, valine.

Fig. 6. Sequenced mass spectra of two different Cu^{2+}-chelating peptides structures obtained from sunflower meal protein isolate hydrolysates and processes by MaxQuant software. (A) **H**NDGNTELVVVVF (F2: Prot+Flav) and (B) SP**H**WTIN (F2: all the hydrolysates), containing His residue in the first and third position from amino terminus, respectively. Prot: Protamex® hydrolysate; Prot+Flav: Protamex® followed by Flavourzyme® hydrolysate; ≤ 1 kDa: 1 kDa ultrafiltrated hydrolysate.

Figures

Fig. 1.

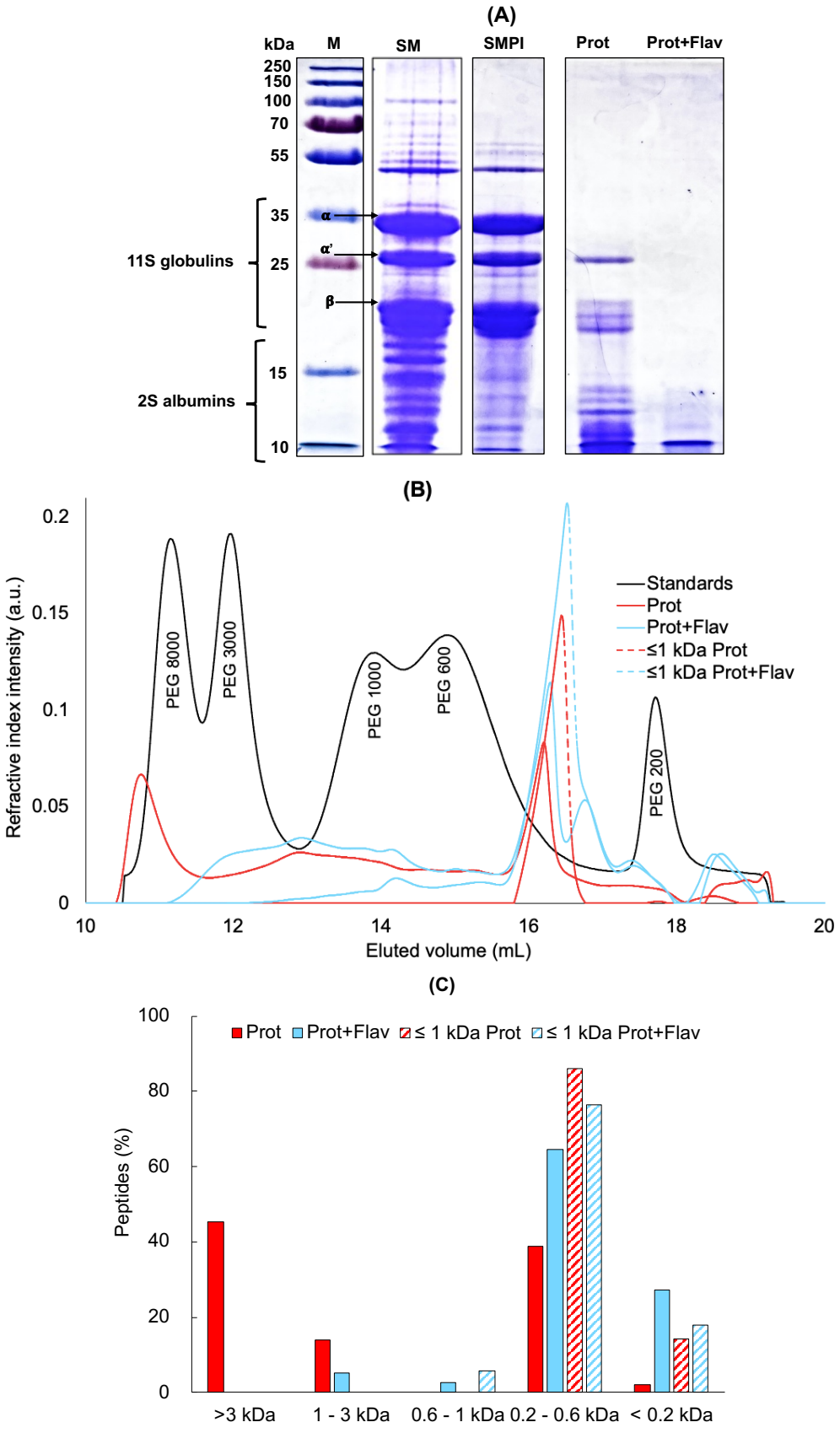

941 **Fig. 2.**

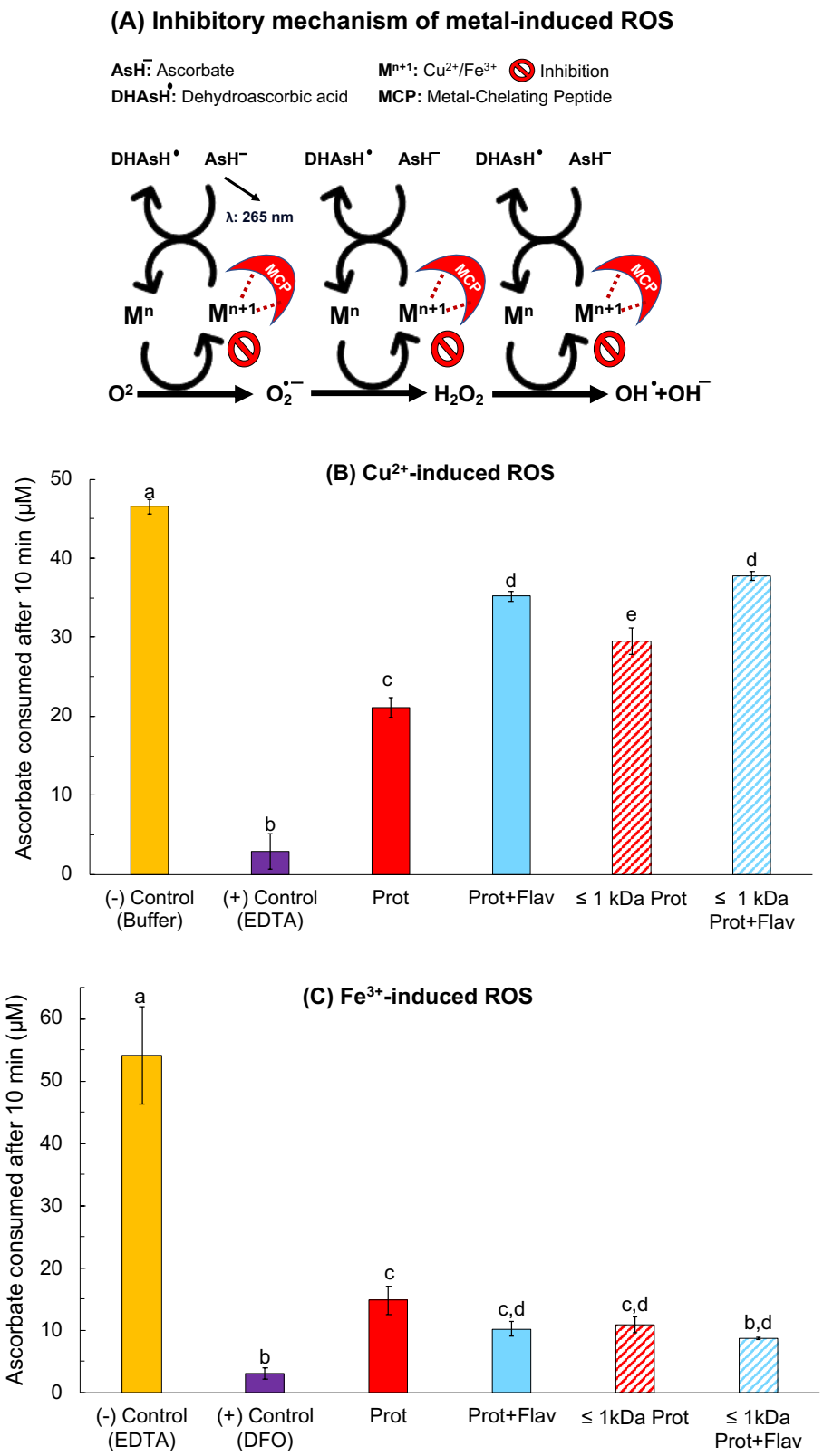

942

943

944

945

946

947

948 **Fig. 3.**

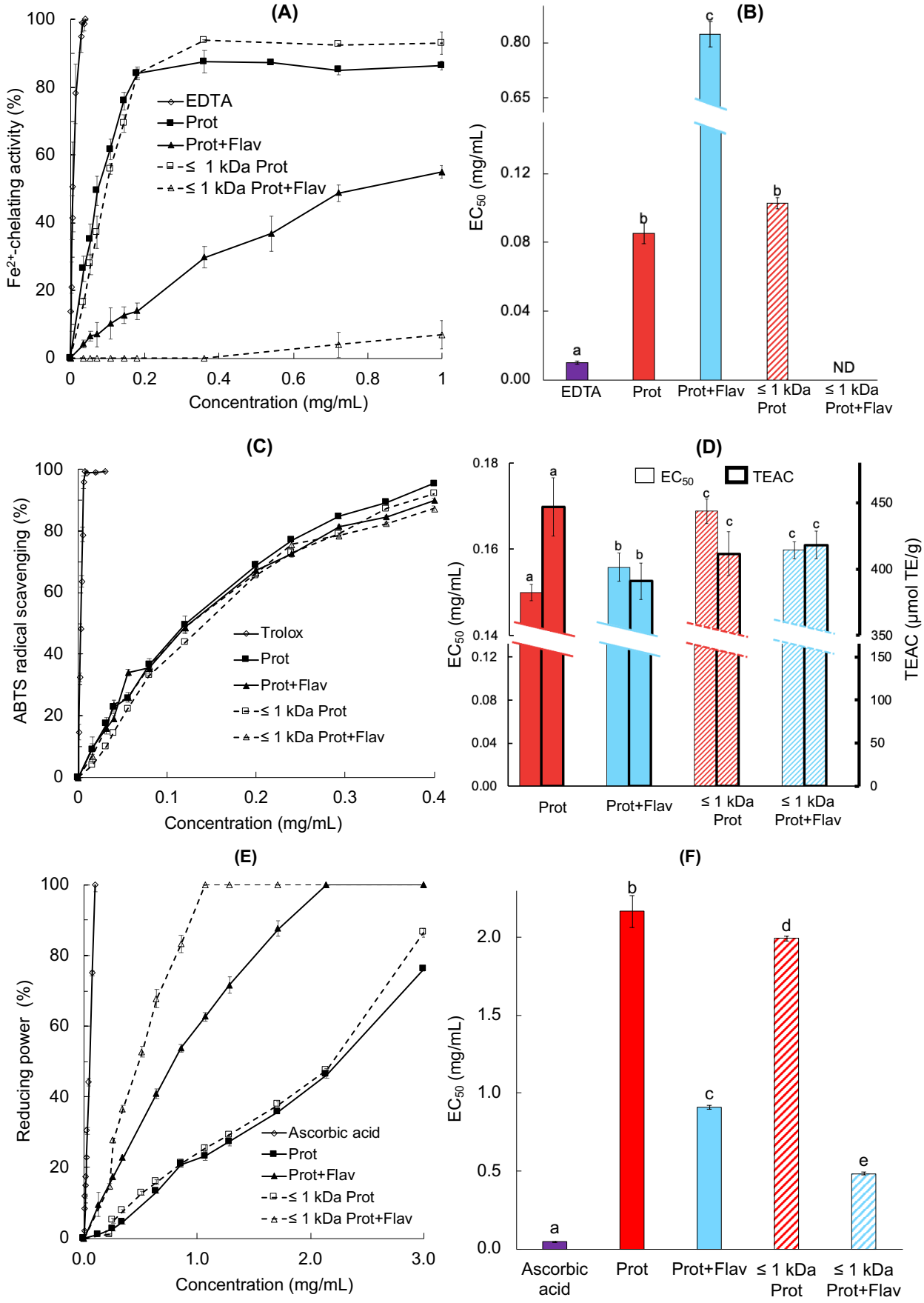

949

950

951

952 **Fig. 4.**

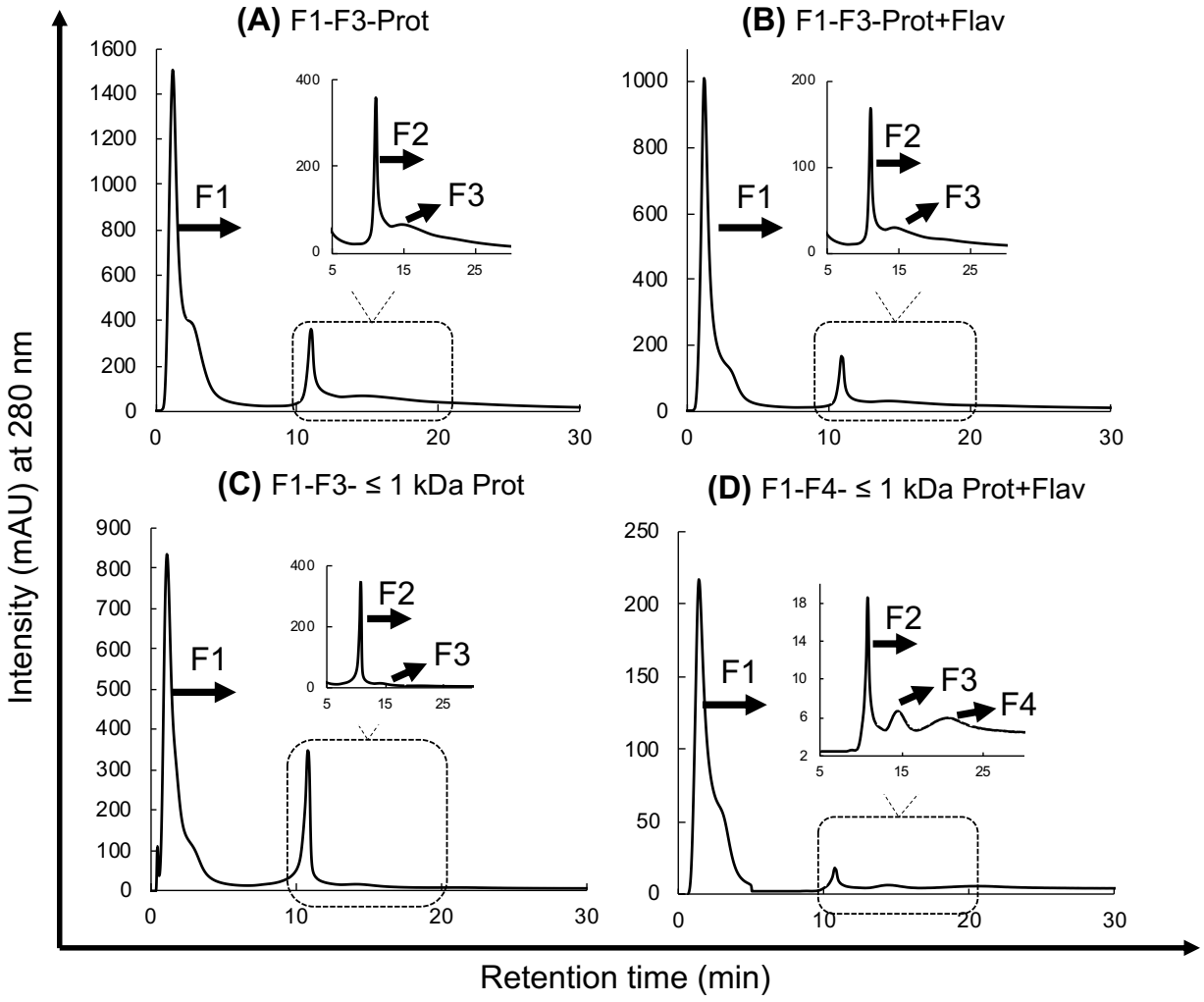

953
954
955
956
957
958
959
960
961
962
963
964
965
966
967
968

Fig. 5.

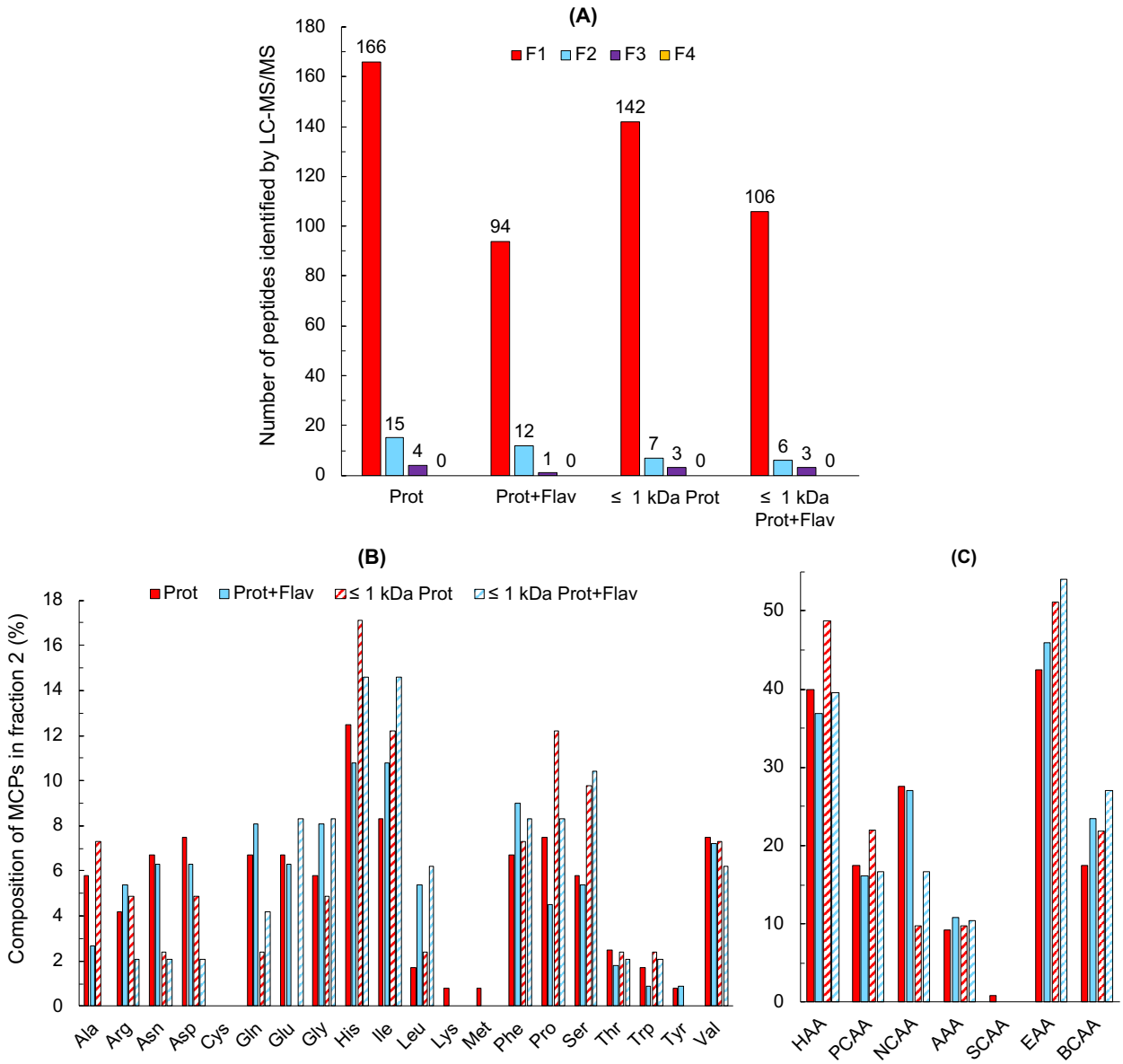
(A)
Number of peptides identified by LC-MS/MS
F1 F2 F3 F4
166
15
4
0
94
12
1
0
142
7
3
0
106
6
3
0
Prot
Prot+Flav
≤ 1 kDa Prot
≤ 1 kDa Prot+Flav
(B)
Prot
Prot+Flav
≤ 1 kDa Prot
≤ 1 kDa Prot+Flav
Composition of MCPs in fraction 2 (%)
Ala
Arg
Asn
Asp
Cys
Gln
Glu
Gly
His
Ile
Leu
Lys
Met
Phe
Pro
Ser
Thr
Trp
Tyr
Val
(C)
HAA
PCAA
NCAA
AAA
SCAA
EAA
BCAA

Fig. 6.

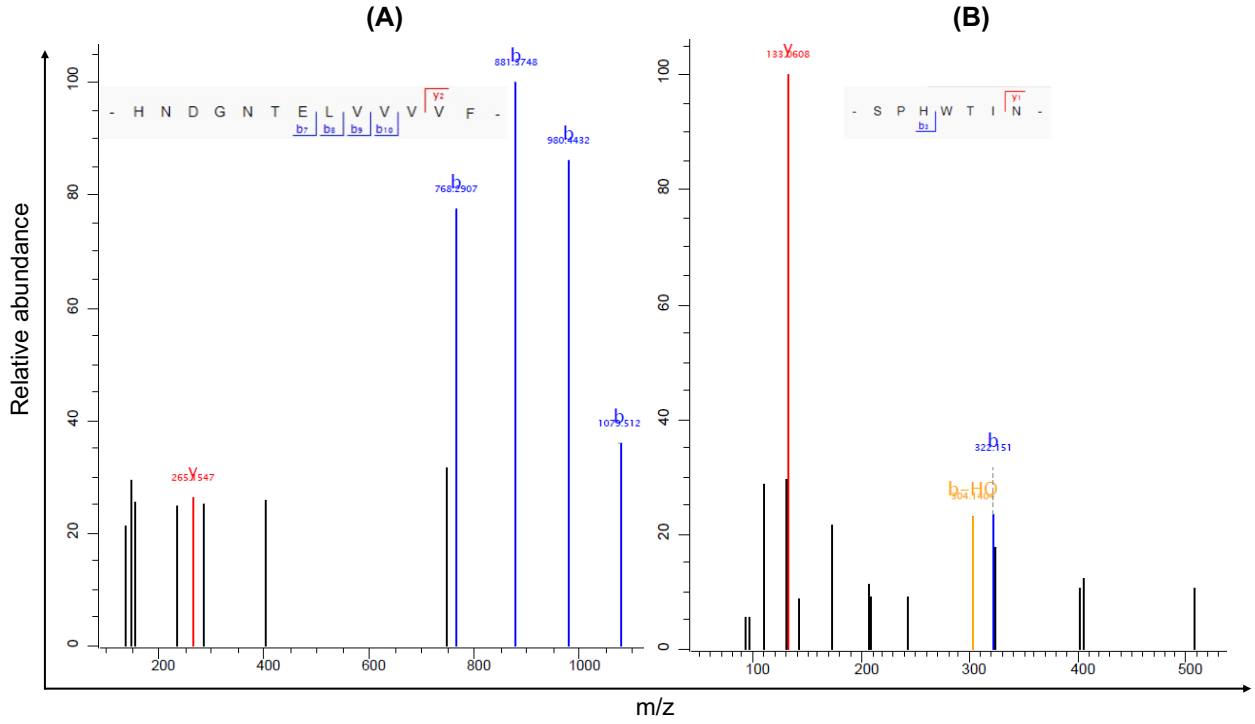
(A)
(B)
- H N D G N T E L V V V V F -
- S P H W T I N -
Relative abundance
m/z
0
20
40
60
80
100
200
400
600
800
1000
100
300
500

1005 **For Table of Contents Only**

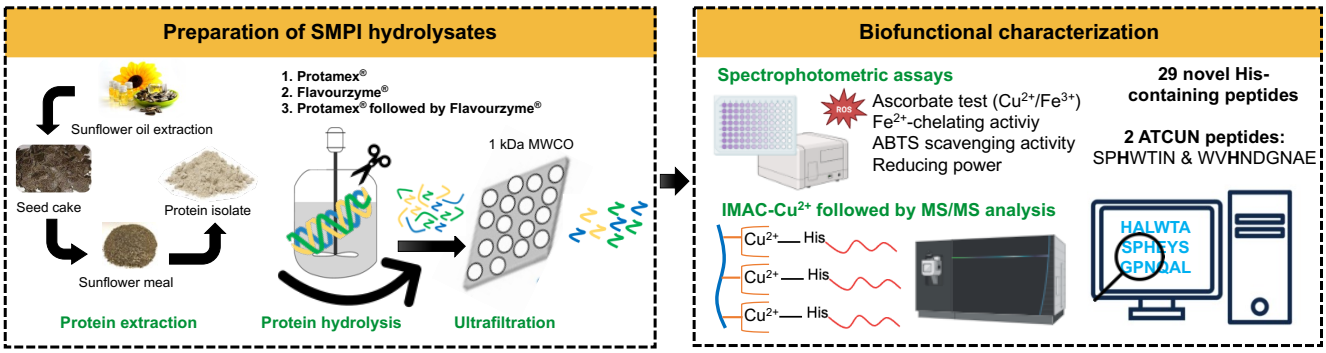

1006

1007